NASA Contractor Report 181979
ICASE Report No. 90–5

ICASE

MODELING THE PRESSURE-STRAIN CORRELATION OF TURBULENCE — AN INVARIANT DYNAMICAL SYSTEMS APPROACH

Charles G. Speziale
Sutanu Sarkar
Thomas B. Gatski

Contract No. NAS1–18605
January 1990

Institute for Computer Applications in Science and Engineering
NASA Langley Research Center
Hampton, Virginia 23665–5225

Operated by the Universities Space Research Association

National Aeronautics and Space Administration

Langley Research Center
Hampton, Virginia 23665-5225

MODELING THE PRESSURE-STRAIN CORRELATION OF TURBULENCE – AN INVARIANT DYNAMICAL SYSTEMS APPROACH

Charles G. Speziale and Sutanu Sarkar*
ICASE, NASA Langley Research Center
Hampton, VA 23665

Thomas B. Gatski
NASA Langley Research Center
Hampton, VA 23665

ABSTRACT

The modeling of the pressure-strain correlation of turbulence is examined from a basic theoretical standpoint with a view toward developing improved second-order closure models. Invariance considerations along with elementary dynamical systems theory are used in the analysis of the standard hierarchy of closure models. In these commonly used models, the pressure-strain correlation is assumed to be a linear function of the mean velocity gradients with coefficients that depend algebraically on the anisotropy tensor. It is proven that for plane homogeneous turbulent flows the equilibrium structure of this hierarchy of models is encapsulated by a relatively simple model which is only quadratically nonlinear in the anisotropy tensor. This new quadratic model – the SSG model – is shown to outperform the Launder, Reece, and Rodi model (as well as more recent models that have a considerably more complex nonlinear structure) in a variety of homogeneous turbulent flows. However, some deficiencies still remain for the description of rotating turbulent shear flows that are intrinsic to this general hierarchy of models and, hence, cannot be overcome by the mere introduction of more complex nonlinearities. It is thus argued that the recent trend of adding substantially more complex nonlinear terms containing the anisotropy tensor may be of questionable value in the modeling of the pressure-strain correlation. Possible alternative approaches are discussed briefly.

*This research was supported by the National Aeronautics and Space Administration under NASA Contract No. NAS1-18605 while the first and second authors were in residence at the Institute for Computer Applications in Science and Engineering (ICASE), NASA Langley Research Center, Hampton, VA 23665.

1. INTRODUCTION

The pressure-strain correlation plays a pivotal role in determining the structure of a wide variety of turbulent flows. Consequently, the proper modeling of this term is essential for the development of second-order closure models that have reliable predictive capabilities. Rotta (1951) developed the first simple model for the slow pressure-strain correlation (i.e., the part that is independent of the mean velocity gradients) which describes the return to isotropy behavior of turbulence within the framework of a full Reynolds stress closure. This model has served as a cornerstone for the representation of the slow pressure-strain correlation in a variety of the commonly used second-order closures such as the Launder, Reece, and Rodi (1975) model. Subsequent to this work, Lumley (1978) demonstrated the need for nonlinear terms in models for the slow pressure-strain correlation and derived a nonlinear representation theorem for the slow pressure-strain correlation based on isotropic tensor function theory. In the high-Reynolds-number and small anisotropy limit, the Lumley (1978) model reduces to the Rotta model.

The simplest model for the rapid pressure-strain correlation that is used in second-order closure modeling is based on the assumption of isotropy of the coefficients of the mean velocity gradients; this gives rise to a rapid pressure-strain model with a single term that is proportional to the mean rate of strain tensor (see Rotta 1972 and Mellor and Herring 1973). Starting with the work of Launder, Reece, and Rodi (1975), anisotropic models for the rapid pressure-strain correlation have been formulated wherein the coefficients of the mean velocity gradients are taken to be functions of the anisotropy tensor. In the Launder, Reece, and Rodi model, the fourth-rank tensor of coefficients of the mean velocity gradient tensor is *linear* in the anisotropy tensor whereas most of the newer models developed during the last decade are nonlinear (see Shih and Lumley 1985, Haworth and Pope 1986, Speziale 1987, Reynolds 1987, and Fu, Launder, and Tselepidakis 1987). The nonlinear models of Lumley and co-workers have been primarily developed by the use of realizability constraints (see Lumley 1978). In contrast to this approach, the nonlinear model of Speziale (1987) was derived using a geostrophic flow constraint (i.e., material frame-indifference in the limit of two-dimensional turbulence) whereas Reynolds (1988) has attempted to develop models that are consistent with Rapid Distortion Theory (RDT).

In this paper, the general hierarchy of closure models for the pressure-strain correlation will be considered which are linear in the mean velocity gradients, with coefficients that are functions of the anisotropy tensor. This hierarchy of models, which was motivated by analyses of homogeneous turbulence, encompasses all of the closure models for the pressure-strain correlation that have been used in connection with second-order closures. A general representation for this hierarchy of closure models will be derived by means of invariant tensor

function theory. This general representation for the pressure-strain correlation will then be applied to plane homogeneous turbulent flows – the class of flows that have long played a pivotal role in the screening and calibration of such models. However, there will be one notable difference with previous work on this subject: the simplest generic form of this hierarchy of models will be sought that has the same equilibrium structure in the phase space of plane homogeneous turbulent flows as the general model. This generic form – which will be termed the SSG model - is only quadratically nonlinear in the anisotropy tensor. It has the advantage of being topologically equivalent to the general model in plane homogeneous turbulence with the simplicity of structure that allows for the determination of all empirical constants based on calibrations with pertinent RDT results and two well documented physical experiments (i.e., homogeneous turbulent shear flow and the decay of isotropic turbulence). This new SSG model will be shown to perform better than the commonly used Launder, Reece, and Rodi model for a variety of homogeneous turbulent flows which include plane strain, rotating plane shear, and the axisymmetric expansion/contraction. However, there are still some remaining deficiencies in the new model, particularly for rotating shear flow. Based on an analysis of the bifurcation diagram for rotating shear flow, it will be shown that these deficiencies are intrinsic to this general hierarchy of pressure-strain models and cannot be eliminated by the addition of more complex nonlinear terms. The implications that these results have on turbulence modeling will be discussed in detail along with suggested future directions of research.

2. THE GENERAL PRESSURE-STRAIN MODEL

We will consider the turbulent flow of a viscous, incompressible fluid governed by the Navier-Stokes and continuity equations

$$\frac{\partial v_i}{\partial t} + v_j \frac{\partial v_i}{\partial x_j} = -\frac{\partial P}{\partial x_i} + \nu \nabla^2 v_i \tag{1}$$

$$\frac{\partial v_i}{\partial x_i} = 0. \tag{2}$$

In (1) - (2), v_i is the velocity vector, P is the modified pressure, and ν is the kinematic viscosity of the fluid. The velocity and pressure are decomposed into ensemble mean and fluctuating parts, respectively, as follows:

$$v_i = \overline{v}_i + u_i, \quad P = \overline{P} + p. \tag{3}$$

Here, the mean and fluctuating velocity are solutions of the transport equations

$$\frac{\partial \overline{v}_i}{\partial t} + \overline{v}_j \frac{\partial \overline{v}_i}{\partial x_j} = -\frac{\partial \overline{P}}{\partial x_i} + \nu \nabla^2 \overline{v}_i + \frac{\partial \tau_{ij}}{\partial x_j} \tag{4}$$

$$\frac{\partial \overline{v}_i}{\partial x_i} = 0 \tag{5}$$

$$\frac{\partial u_i}{\partial t} + \overline{v}_j \frac{\partial u_i}{\partial x_j} = -u_j \frac{\partial u_i}{\partial x_j} - u_j \frac{\partial \overline{v}_i}{\partial x_j} - \frac{\partial p}{\partial x_i} + \nu \nabla^2 u_i - \frac{\partial \tau_{ij}}{\partial x_j} \tag{6}$$

$$\frac{\partial u_i}{\partial x_i} = 0 \tag{7}$$

where $\tau_{ij} \equiv -\overline{u_i u_j}$ is the Reynolds stress tensor.

The Reynolds stress tensor τ_{ij} is a solution of the transport equation

$$\frac{\partial \tau_{ij}}{\partial t} + \overline{v}_k \frac{\partial \tau_{ij}}{\partial x_k} = -\tau_{ik} \frac{\partial \overline{v}_j}{\partial x_k} - \tau_{jk} \frac{\partial \overline{v}_i}{\partial x_k} + \frac{\partial C_{ijk}}{\partial x_k} - \Pi_{ij} + \varepsilon_{ij} + \nu \nabla^2 \tau_{ij} \tag{8}$$

where

$$C_{ijk} \equiv \overline{u_i u_j u_k} + \overline{p u_i} \delta_{jk} + \overline{p u_j} \delta_{ik} \tag{9}$$

$$\Pi_{ij} = \overline{p \left(\frac{\partial u_i}{\partial x_j} + \frac{\partial u_j}{\partial x_i} \right)} \tag{10}$$

$$\varepsilon_{ij} = 2\nu \overline{\frac{\partial u_i}{\partial x_k} \frac{\partial u_j}{\partial x_k}} \tag{11}$$

are, respectively, the third-order diffusion correlation, the pressure-strain correlation, and the dissipation rate correlation. Equation (8) is obtained by taking the symmetric part of the ensemble mean of the product of the fluctuating velocity u_j with equation (6). For homogeneous turbulent flows, at high Reynolds numbers where the dissipation is approximately isotropic, the Reynolds stress transport equation (8) simplifies to

$$\dot{\tau}_{ij} = -\tau_{ik} \frac{\partial \overline{v}_j}{\partial x_k} - \tau_{jk} \frac{\partial \overline{v}_i}{\partial x_k} - \Pi_{ij} + \frac{2}{3} \varepsilon \delta_{ij} \tag{12}$$

where

$$\varepsilon = \nu \overline{\frac{\partial u_i}{\partial x_k} \frac{\partial u_i}{\partial x_k}} \tag{13}$$

is the scalar dissipation rate. Equation (12) becomes a closed system for the determination of τ_{ij} in terms of $\partial \overline{v}_i / \partial x_j$ once closure models for Π_{ij} and ε are provided. Since Π_{ij} is the only unknown correlation that contains *directional information*, it is clear that it will play a pivotal role in determining the structure of the Reynolds stress tensor for a given mean velocity field. This dominant influence of Π_{ij} on the evolution of the Reynolds stress tensor in (12) has motivated researchers to rely on homogeneous turbulent flows for the testing and calibration of pressure-strain models.

The fluctuating pressure p is a solution of the Poisson equation

$$\nabla^2 p = -2 \frac{\partial u_j}{\partial x_i} \frac{\partial \overline{v}_i}{\partial x_j} - \frac{\partial u_i}{\partial x_j} \frac{\partial u_j}{\partial x_i} + \overline{\frac{\partial u_i}{\partial x_j} \frac{\partial u_j}{\partial x_i}} \tag{14}$$

which is obtained by subtracting the divergence of (4) from the divergence of (1). In the absence of boundaries, equation (14) has the general solution

$$p = \frac{1}{4\pi}\int_{-\infty}^{\infty}\frac{1}{|\mathbf{x}-\mathbf{x}'|}\left(2\frac{\partial u_j'}{\partial x_i'}\frac{\partial \overline{v}_i'}{\partial x_j'} + \frac{\partial u_i'}{\partial x_j'}\frac{\partial u_j'}{\partial x_i'} - \overline{\frac{\partial u_i'}{\partial x_j'}\frac{\partial u_j'}{\partial x_i'}}\right)dV'. \tag{15}$$

For homogeneous turbulent flows (where the mean velocity gradients are spatially uniform) the pressure-strain correlation takes the form

$$\Pi_{ij} = A_{ij} + M_{ijk\ell}\frac{\partial \overline{v}_k}{\partial x_\ell} \tag{16}$$

where

$$A_{ij} = \frac{1}{4\pi}\int_{-\infty}^{\infty}\overline{\left(\frac{\partial u_i}{\partial x_j} + \frac{\partial u_j}{\partial x_i}\right)\frac{\partial^2 u_k' u_\ell'}{\partial x_k' \partial x_\ell'}\frac{dV'}{|\mathbf{x}'-\mathbf{x}|}} \tag{17}$$

$$M_{ijk\ell} = \frac{1}{2\pi}\int_{-\infty}^{\infty}\overline{\left(\frac{\partial u_i}{\partial x_j} + \frac{\partial u_j}{\partial x_i}\right)\frac{\partial u_\ell'}{\partial x_k'}\frac{dV'}{|\mathbf{x}'-\mathbf{x}|}}. \tag{18}$$

It has been shown that A_{ij} and $M_{ijk\ell}$ are functionals – over time and wavenumber space – of the energy spectrum tensor; see Weinstock (1981, 1982) and Reynolds (1987). In a one point closure, this dependence would suggest models for A_{ij} and $M_{ijk\ell}$ that depend on the history of the Reynolds stress tensor and dissipation rate. The simplest such models are algebraic in form:

$$A_{ij} = \varepsilon \mathcal{A}_{ij}(\mathbf{b}) \tag{19}$$

$$M_{ijk\ell} = K\mathcal{M}_{ijk\ell}(\mathbf{b}) \tag{20}$$

where

$$b_{ij} \equiv \frac{\tau_{ij} - \frac{1}{3}\tau_{kk}\delta_{ij}}{\tau_{\ell\ell}} \tag{21}$$

$$K = -\frac{1}{2}\tau_{kk} \tag{22}$$

are the anisotropy tensor and turbulent kinetic energy. In (19) - (20), $\mathcal{A}_{ij}$ and $\mathcal{M}_{ijk\ell}$ can only depend on τ_{ij} through b_{ij} since they are dimensionless tensors that vanish in the limit of isotropic turbulence. Virtually *all* models for the pressure-strain correlation that have been used in connection with second-order closure models are of the general form of (19) - (20). The use of this hierarchy of models for general inhomogeneous turbulent flows is based on the assumption of a local homogeneous structure.

The mean velocity gradient tensor can be decomposed into symmetric and antisymmetric parts as follows:

$$\frac{\partial \overline{v}_i}{\partial x_j} = \overline{S}_{ij} + \overline{\omega}_{ij} \tag{23}$$

where

$$\overline{S}_{ij} = \frac{1}{2}\left(\frac{\partial \overline{v}_i}{\partial x_j} + \frac{\partial \overline{v}_j}{\partial x_i}\right) \tag{24}$$

$$\overline{\omega}_{ij} = \frac{1}{2}\left(\frac{\partial \overline{v}_i}{\partial x_j} - \frac{\partial \overline{v}_j}{\partial x_i}\right) \tag{25}$$

are the mean rate of strain tensor and mean vorticity tensor, respectively. Then, the model for the pressure-strain correlation specified by (19) - (20) can be written in the equivalent form

$$\Pi_{ij} = \varepsilon f_{ij}^{(L)}(\mathbf{b}, \overline{\mathbf{S}}', \overline{\omega}') \tag{26}$$

where

$$\overline{S}'_{ij} = \frac{K}{\varepsilon}\overline{S}_{ij}, \quad \overline{\omega}'_{ij} = \frac{K}{\varepsilon}\overline{\omega}_{ij} \tag{27}$$

are the dimensionless mean strain rate and vorticity tensor whereas $f_{ij}^{(L)}$ denotes the part of the function f_{ij} that is *linear* in the mean velocity gradients and traceless. Form invariance under a change of coordinates requires that f_{ij} transform as

$$\mathbf{Q}\mathbf{f}(\mathbf{b}, \overline{\mathbf{S}}', \overline{\omega}')\mathbf{Q}^T = \mathbf{f}(\mathbf{Q}\mathbf{b}\mathbf{Q}^T, \mathbf{Q}\overline{\mathbf{S}}'\mathbf{Q}^T, \mathbf{Q}\overline{\omega}'\mathbf{Q}^T) \tag{28}$$

where $\mathbf{Q}$ is the rotation tensor (and $\mathbf{Q}^T$ is its transpose) which characterizes a change in orientation of the coordinate axes. In mathematical terms, (28) requires that f_{ij} be an isotropic tensor function of its arguments. By using known representation theorems for isotropic tensor functions (see Smith 1971) to construct f_{ij} – and then by taking the linear and traceless part of f_{ij} – the following model for Π_{ij} is obtained:

$$\begin{aligned}
\Pi_{ij} \;=\; & \beta_1 \varepsilon b_{ij} + \beta_2 \varepsilon (b_{ik}b_{kj} - \frac{1}{3} b_{mn}b_{mn}\delta_{ij}) + \beta_3 K \overline{S}_{ij} \\
& + \beta_4 K (b_{ik}\overline{S}_{jk} + b_{jk}\overline{S}_{ik} - \frac{2}{3} b_{mn}\overline{S}_{mn}\delta_{ij}) \\
& + \beta_5 K (b_{ik}b_{k\ell}\overline{S}_{j\ell} + b_{jk}b_{k\ell}\overline{S}_{i\ell} - \frac{2}{3} b_{\ell m}b_{mn}\overline{S}_{n\ell}\delta_{ij}) \\
& + \beta_6 K (b_{ik}\overline{\omega}_{jk} + b_{jk}\overline{\omega}_{ik}) + \beta_7 K (b_{ik}b_{k\ell}\overline{\omega}_{j\ell} + b_{jk}b_{k\ell}\overline{\omega}_{i\ell})
\end{aligned} \tag{29}$$

where

$$\beta_i = \beta_{i0}(II, III) + \beta_{i1}(II, III)\frac{K}{\varepsilon} tr(\mathbf{b}\cdot\overline{\mathbf{S}}) + \beta_{i2}(II, III)\frac{K}{\varepsilon} tr(\mathbf{b}^2\cdot\overline{\mathbf{S}}), \quad i = 1, 2 \tag{30}$$

$$\beta_j = \beta_j(II, III), \quad j = 3, 4, \ldots, 7 \tag{31}$$

$$II = b_{ij}b_{ij}, \quad III = b_{ij}b_{jk}b_{ki} \tag{32}$$

and $tr(\cdot)$ denotes the trace (see Appendix A for more details). Equation (29) represents the *most general form* of the hierarchy of models (19) - (20) for the pressure-strain correlation that is consistent with the crucial physical constraint of invariance under coordinate transformations. It will be shown later that the Launder, Reece, and Rodi model is the linear limit of (29) wherein $\beta_1, \beta_3, \beta_4$, and β_6 are constants while β_2, β_5, and β_7 are zero.

Finally, in regard to the general model, a few comments should be made concerning non-inertial frames of reference. In a non-inertial frame, the mean vorticity tensor $\overline{\omega}_{ij}$ must be replaced by the intrinsic (i.e., absolute) mean vorticity tensor defined by

$$\overline{W}_{ij} = \overline{\omega}_{ij} + e_{mji}\Omega_m \tag{33}$$

where Ω_m is the rotation rate of the non-inertial frame relative to an inertial framing and e_{mji} is the permutation tensor (see Launder, Tselepidakis, and Younis 1987 and Speziale 1989a). Furthermore, Coriolis terms must be added to the Reynolds stress transport equation which then takes the form

$$\mathring{\tau}_{ij} = -\tau_{ik}\frac{\partial \overline{v}_j}{\partial x_k} - \tau_{jk}\frac{\partial \overline{v}_i}{\partial x_k} - \Pi_{ij} + \frac{2}{3}\varepsilon\delta_{ij} - 2(\tau_{ik}e_{mkj}\Omega_m + \tau_{jk}e_{mki}\Omega_m) \tag{34}$$

in an arbitrary non-inertial reference frame.

3. PLANE HOMOGENEOUS TURBULENCE

We will consider the general class of plane homogeneous turbulent flows for which the mean velocity gradient tensor can be written in the form

$$\frac{\partial \overline{v}_i}{\partial x_j} = \begin{pmatrix} 0 & S+\omega & 0 \\ S-\omega & 0 & 0 \\ 0 & 0 & 0 \end{pmatrix}. \tag{35}$$

Since the mean continuity equation (5) requires that $\partial \overline{v}_1/\partial x_1 = -\partial \overline{v}_2/\partial x_2$ in plane homogeneous turbulent flows, equation (35) results by simply aligning the coordinates at a 45° angle relative to the principal directions of the symmetric part of $\partial \overline{v}_i/\partial x_j$. Of course, in order to maintain the homogeneity and two-dimensionality of the mean flow, S and ω are constants while Ω_i is given by

$$\Omega_i = (0, 0, \Omega) \tag{36}$$

(hence, the rotation is in the plane where the mean velocity gradients are applied). Equations (35) - (36) encompass, as special cases, plane shear, plane strain, rotating plane shear, and rotating plane strain turbulence.

The Reynolds stress transport equation (34) for plane homogeneous turbulence can be written in terms of the anisotropy tensor $b_{ij}(t^*)$ (given that $t^* \equiv St$ is the dimensionless time) as follows:

$$\begin{aligned}\frac{db_{ij}}{dt^*} &= \frac{\varepsilon}{SK}\left(1-\frac{\mathcal{P}}{\varepsilon}\right)b_{ij} - b_{ik}(\overline{S}^*_{jk} + \overline{\omega}^*_{jk} \\ &\quad +2\frac{\Omega}{S}e_{3kj}) - b_{jk}(\overline{S}^*_{ik} + \overline{\omega}^*_{ik} + 2\frac{\Omega}{S}e_{3ki}) \\ &\quad -\frac{1}{3}\frac{\mathcal{P}}{\varepsilon}\left(\frac{\varepsilon}{SK}\right)\delta_{ij} - \frac{2}{3}\overline{S}^*_{ij} + \Pi^*_{ij}\end{aligned} \tag{37}$$

where

$$\overline{S}^*_{ij} = \begin{pmatrix} 0 & 1 & 0 \\ 1 & 0 & 0 \\ 0 & 0 & 0 \end{pmatrix}, \quad \overline{\omega}^*_{ij} = \begin{pmatrix} 0 & \frac{\omega}{S} & 0 \\ -\frac{\omega}{S} & 0 & 0 \\ 0 & 0 & 0 \end{pmatrix}, \tag{38}$$

$$\Pi^*_{ij} = \Pi_{ij}/2KS \tag{39}$$

and $\mathcal{P} \equiv \tau_{ij}\partial\overline{v}_i/\partial x_j$ is the turbulence production. Equation (37) must be supplemented with a transport model for the turbulent dissipation rate in order to obtain a closed system. We will consider the most standard form of the modeled dissipation rate transport equation given by

$$\dot{\varepsilon} = C_{\varepsilon 1}\frac{\varepsilon}{K}\tau_{ij}\frac{\partial\overline{v}_i}{\partial x_j} - C_{\varepsilon 2}\frac{\varepsilon^2}{K} \tag{40}$$

where $C_{\varepsilon 1}$ and $C_{\varepsilon 2}$ can be functions of the invariants II and III of the anisotropy tensor (in the most commonly used form of this model, $C_{\varepsilon 1}$ and $C_{\varepsilon 2}$ are constants that assume the values of 1.44 and 1.92, respectively; see Hanjalic and Launder 1972). It will be argued later that some of the crucial conclusions to be drawn concerning the limitations of this hierarchy of closure models for the pressure-strain correlation are independent of the specific form of (40). Furthermore, it should be noted that virtually all of the alterations to (40) that have been proposed during the last decade are highly ill-behaved (see Speziale 1989b).

The modeled dissipation rate equation (40) can be written in the dimensionless form

$$\frac{d}{dt^*}\left(\frac{\varepsilon}{SK}\right) = \left(\frac{\varepsilon}{SK}\right)^2[(C_{\varepsilon 1}-1)\frac{\mathcal{P}}{\varepsilon} - (C_{\varepsilon 2}-1)]. \tag{41}$$

Equation (41) is obtained by combining (40) with the transport equation for the turbulent kinetic energy

$$\dot{K} = \mathcal{P} - \varepsilon \tag{42}$$

which is exact for homogeneous turbulence. When the general model for the pressure-strain correlation (given by (29), with $\overline{\omega}_{ij}$ replaced by $\overline{W}_{ij}$) is substituted into (37), a closed system

for the determination of b_{ij} and ε/SK is obtained. This system of equations has equilibrium solutions of the form

$$(b_{ij})_\infty = g_{ij}\left(\frac{\omega}{S}, \frac{\Omega}{S}\right) \tag{43}$$

$$\left(\frac{\varepsilon}{SK}\right)_\infty = g\left(\frac{\omega}{S}, \frac{\Omega}{S}\right) \tag{44}$$

where $(\cdot)_\infty$ denotes the solution in the limit as time $t \to \infty$; these solutions were shown by Speziale and Mac Giolla Mhuiris (1989a) to attract *all initial conditions*. The equilibrium solutions (43) - (44) are obtained by solving the nonlinear algebraic equations that result when the time derivatives on the left-hand-sides of (37) and (41) are set to zero. It is a simple matter to show that there is a trivial equilibrium solution where

$$\left(\frac{\varepsilon}{SK}\right)_\infty = 0 \tag{45}$$

which exists for all ω/S and Ω/S. Non-trivial equilibrium solutions where $(\varepsilon/SK)_\infty \neq 0$ exist for intermediate ranges of ω/S and Ω/S wherein the trivial equilibrium solution (45) typically becomes unstable.

We will now show that the non-trivial equilibrium values of $II_\infty, III_\infty, (b_{33})_\infty$, and $(\mathcal{P}/\varepsilon)_\infty$ are *universal* (i.e., completely independent of ω/S and Ω/S) for this hierarchy of models in plane homogeneous turbulent flows. A closed system of equations for the determination of the temporal evolution of *II*, *III*, b_{33} and ε/SK are as follows:

$$\begin{aligned}
\frac{dII}{dt^*} &= \frac{2\varepsilon}{SK}\left(1 - \frac{\mathcal{P}}{\varepsilon}\right) II - 2b_{33}\frac{\mathcal{P}}{\varepsilon}\frac{\varepsilon}{SK} + \frac{2}{3}\frac{\mathcal{P}}{\varepsilon}\frac{\varepsilon}{SK} \\
&\quad + \beta_1 \frac{\varepsilon}{SK} II + \beta_2 \frac{\varepsilon}{SK} III - \frac{1}{2}\beta_3 \frac{\mathcal{P}}{\varepsilon}\frac{\varepsilon}{SK} \\
&\quad + \beta_4 b_{33}\frac{\mathcal{P}}{\varepsilon}\frac{\varepsilon}{SK} - \frac{1}{2}\beta_5 II \frac{\mathcal{P}}{\varepsilon}\frac{\varepsilon}{SK}
\end{aligned} \tag{46}$$

$$\begin{aligned}
\frac{dIII}{dt^*} &= \frac{3\varepsilon}{SK}\left(1 - \frac{\mathcal{P}}{\varepsilon}\right) III + \frac{3}{2} II \frac{\mathcal{P}}{\varepsilon}\frac{\varepsilon}{SK} - II\frac{\mathcal{P}}{\varepsilon}\frac{\varepsilon}{SK} \\
&\quad - b_{33}\frac{\mathcal{P}}{\varepsilon}\frac{\varepsilon}{SK} + \frac{3}{2}\beta_1 III \frac{\varepsilon}{SK} + \frac{1}{4}\beta_2 II^2 \frac{\varepsilon}{SK} \\
&\quad + \frac{3}{4}\beta_3 b_{33}\frac{\mathcal{P}}{\varepsilon}\frac{\varepsilon}{SK} - \frac{1}{4}\beta_4 II \frac{\mathcal{P}}{\varepsilon}\frac{\varepsilon}{SK} \\
&\quad + \frac{1}{4}\beta_5 II b_{33}\frac{\mathcal{P}}{\varepsilon}\frac{\varepsilon}{SK} - \frac{1}{2}\beta_5 III \frac{\mathcal{P}}{\varepsilon}\frac{\varepsilon}{SK}
\end{aligned} \tag{47}$$

$$\begin{aligned}\frac{db_{33}}{dt^*} &= \frac{\varepsilon}{SK}\left(1-\frac{\mathcal{P}}{\varepsilon}\right)b_{33}-\frac{1}{3}\frac{\mathcal{P}}{\varepsilon}\frac{\varepsilon}{SK} \\ &+\frac{1}{2}\beta_1\frac{\varepsilon}{SK}b_{33}+\frac{1}{2}\beta_2\frac{\varepsilon}{SK}\left(b_{33}^2-\frac{1}{3}II\right)\end{aligned} \tag{48}$$

$$\frac{d}{dt^*}\left(\frac{\varepsilon}{SK}\right)=\left(\frac{\varepsilon}{SK}\right)^2\left[(C_{\varepsilon 1}-1)\frac{\mathcal{P}}{\varepsilon}-(C_{\varepsilon 2}-1)\right]. \tag{49}$$

Equations (46) - (47) are obtained by multiplying (37) with $\mathbf{b}$ and $\mathbf{b}^2$, respectively, and then taking the trace after the model (29) for Π_{ij} is substituted. The non-trivial equilibrium solutions are then obtained from the nonlinear algebraic equations

$$\begin{aligned}&2\left[1-\left(\frac{\mathcal{P}}{\varepsilon}\right)_\infty\right]II_\infty-2(b_{33})_\infty\left(\frac{\mathcal{P}}{\varepsilon}\right)_\infty+\frac{2}{3}\left(\frac{\mathcal{P}}{\varepsilon}\right)_\infty \\ &+\beta_1 II_\infty+\beta_2 III_\infty-\frac{1}{2}\beta_3\left(\frac{\mathcal{P}}{\varepsilon}\right)_\infty+\beta_4(b_{33})_\infty\left(\frac{\mathcal{P}}{\varepsilon}\right)_\infty \\ &-\frac{1}{2}\beta_5 II_\infty\left(\frac{\mathcal{P}}{\varepsilon}\right)_\infty=0\end{aligned} \tag{50}$$

$$\begin{aligned}&3\left[1-\left(\frac{\mathcal{P}}{\varepsilon}\right)_\infty\right]III_\infty+\frac{3}{2}II_\infty\left(\frac{\mathcal{P}}{\varepsilon}\right)_\infty-II_\infty\left(\frac{\mathcal{P}}{\varepsilon}\right)_\infty \\ &-(b_{33})_\infty\left(\frac{\mathcal{P}}{\varepsilon}\right)_\infty+\frac{3}{2}\beta_1 III_\infty+\frac{1}{4}\beta_2 II_\infty^2 \\ &+\frac{3}{4}\beta_3(b_{33})_\infty\left(\frac{\mathcal{P}}{\varepsilon}\right)_\infty-\frac{1}{4}\beta_4 II_\infty\left(\frac{\mathcal{P}}{\varepsilon}\right)_\infty \\ &+\frac{1}{4}\beta_5 II_\infty(b_{33})_\infty\left(\frac{\mathcal{P}}{\varepsilon}\right)_\infty-\frac{1}{2}\beta_5 III_\infty\left(\frac{\mathcal{P}}{\varepsilon}\right)_\infty=0\end{aligned} \tag{51}$$

$$\begin{aligned}&\left[1-\left(\frac{\mathcal{P}}{\varepsilon}\right)_\infty\right](b_{33})_\infty-\frac{1}{3}\left(\frac{\mathcal{P}}{\varepsilon}\right)_\infty+\frac{1}{2}\beta_1(b_{33})_\infty \\ &+\frac{1}{2}\beta_2\left[(b_{33})_\infty^2-\frac{1}{3}II_\infty\right]=0\end{aligned} \tag{52}$$

$$(C_{\varepsilon 1}-1)\left(\frac{\mathcal{P}}{\varepsilon}\right)_\infty-(C_{\varepsilon 2}-1)=0 \tag{53}$$

which are derived by setting the time derivatives on the left-hand-sides of (46) - (49) to zero and dividing by ε/SK. The system of equations (50) - (53) will have solutions for

$II_\infty, III_\infty, (b_{33})_\infty$ and $(\mathcal{P}/\varepsilon)_\infty$ that are completely independent of ω/S and Ω/S – and hence universal – for plane homogeneous turbulent flows.

This universal equilibrium structure of $II_\infty, III_\infty, (b_{33})_\infty$ and $(\mathcal{P}/\varepsilon)_\infty$ will now be utilized to obtain the simplest generic form of (29) that has the same equilibrium structure as the general model in the phase space of plane homogeneous turbulent flows. Due to these four universal invariants, the quadratic terms in the rapid pressure strain correlation are *not linearly independent* for plane homogeneous turbulent flows. This quadratic part $\Pi_{ij}^{(2)}$ of (29) is defined as follows:

$$\Pi_{ij}^{(2)} = \beta_5 K(b_{ik}b_{k\ell}\overline{S}_{j\ell} + b_{jk}b_{k\ell}\overline{S}_{i\ell} - \frac{2}{3}b_{\ell m}\overline{S}_{mn}\overline{S}_{n\ell}\delta_{ij}) + \beta_7 K(b_{ik}b_{k\ell}\overline{W}_{j\ell} + b_{jk}b_{k\ell}\overline{W}_{i\ell}). \quad (54)$$

For plane homogeneous turbulent flows, a straightforward, although somewhat tedious, calculation yields the relationships

$$b_{ik}b_{k\ell}\overline{S}_{j\ell} + b_{jk}b_{k\ell}\overline{S}_{i\ell} - \frac{2}{3}b_{k\ell}b_{\ell m}\overline{S}_{mk}\delta_{ij} = -b_{33}(b_{ik}\overline{S}_{jk} + b_{jk}\overline{S}_{ik} - \frac{2}{3}b_{k\ell}\overline{S}_{k\ell}\delta_{ij}) - \frac{2}{3}\frac{III}{b_{33}}\overline{S}_{ij} \quad (55)$$

$$b_{ik}b_{k\ell}\overline{W}_{j\ell} + b_{jk}b_{k\ell}\overline{W}_{i\ell} = -b_{33}(b_{ik}\overline{W}_{jk} + b_{jk}\overline{W}_{ik}) \quad (56)$$

where we have made use of (38) and the fact that the anistropy tensor is of the form

$$b_{ij} = \begin{pmatrix} b_{11} & b_{12} & 0 \\ b_{12} & b_{22} & 0 \\ 0 & 0 & b_{33} \end{pmatrix} \quad (57)$$

in such flows. Due to (55) - (56), and the fact that $II_\infty, III_\infty, (b_{33})_\infty$ and $(\mathcal{P}/\varepsilon)_\infty$ are universal invariants for all plane homogeneous turbulent flows, it follows that the quadratic terms in the rapid pressure-strain are directly related to the linear terms in such flows. Consequently, the equilibrium structure of (29) in plane homogeneous turbulent flows will be indistinguishable from that of the substantially simpler model

$$\begin{aligned} \Pi_{ij} \;=\; & c_1\varepsilon b_{ij} + c_2\varepsilon(b_{ik}b_{kj} - \frac{1}{3}b_{mn}b_{mn}\delta_{ij}) \\ & + c_3 K\,\overline{S}_{ij} + c_4 K(b_{ik}\overline{S}_{jk} + b_{jk}\overline{S}_{ik} \\ & - \frac{2}{3}b_{mn}\overline{S}_{mn}\delta_{ij}) + c_5 K(b_{ik}\overline{W}_{jk} + b_{jk}\overline{W}_{ik}) \end{aligned} \quad (58)$$

where $c_1, c_2, \ldots, c_5$ are dimensionless constants and we have made use of the fact that

$$tr(\mathbf{b}\cdot\overline{\mathbf{S}}) = -\frac{1}{2}\frac{\mathcal{P}}{K} \quad (59)$$

$$tr(\mathbf{b}^2\cdot\overline{\mathbf{S}}) = \frac{1}{2}b_{33}\frac{\mathcal{P}}{K} \quad (60)$$

which was also used in the derivation of (46) - (49). In alternative terms, (58) is topologically equivalent to the general model (29) in so far as the equilibrium structure of plane homogeneous turbulent flows is concerned.

It is rather striking that an analysis of the equilibrium states of arbitrary plane homogeneous turbulence – coupled with the crucial physical constraint of invariance under coordinate transformations – collapses the general pressure-strain model

$$\Pi_{ij} = \varepsilon \mathcal{A}_{ij}(\mathbf{b}) + K\mathcal{M}_{ijk\ell}(\mathbf{b})\frac{\partial \overline{v}_k}{\partial x_\ell}, \tag{61}$$

(which can have as many as forty-five independent functions of $\mathbf{b}$) to the substantially simplified model (58) that has only five undetermined constants. In the next section, a new model for the pressure-strain correlation will be developed.

4. THE SSG MODEL: ITS ASYMPTOTIC ANALYSIS AND CALIBRATION

Now, a new model for the pressure-strain correlation – which we will call the SSG model – will be developed based on the previous invariant dynamical systems analysis coupled with the following additional constraints:

(i) Asymptotic consistency in the limit of small anisotropies

(ii) Consistency with Rapid Distortion Theory for homogeneously strained turbulent flows that are initially isotropic

(iii) Consistency with the equilibrium values for homogeneous shear flow obtained from the physical experiments of Tavoularis and Corrsin (1981)

(iv) Consistency with the RDT results of Bertoglio (1982), for rotating shear flows, which predict that the most unstable flow occurs when the ratio of the rotation rate to the shear rate $\Omega/S = 0.25$ and that a flow restabilization occurs when $\Omega/S > 0.5$

(v) Consistency with the results of physical experiments on the decay of isotropic turbulence and the return to isotropy of an initially anisotropic, homogeneous turbulence.

Since the magnitude of the anisotropy tensor is relatively small ($\|\mathbf{b}\| \leq 0.20$ for most turbulent flows of engineering and scientific interest), we feel that terms which are of a comparable order of magnitude in b_{ij} should be maintained unless there is some overriding physical reason not to do so. In this fashion, the model can then be thought of as an asymptotically consistent truncation of a Taylor series expansion of A_{ij} and $M_{ijk\ell}$ in the variable b_{ij}. Since

the simplified model for the rapid pressure-strain correlation in (58) is of $\mathcal{O}(\mathbf{b})$, this suggests that c_3 – which in general can be a function of the invariants of $\mathbf{b}$ – should be replaced by

$$C_3 - C_3^* II^{\frac{1}{2}}$$

(where C_3 and C_3^* are constants) for asymptotic consistency. Furthermore, since the model for the slow pressure-strain correlation is of $\mathcal{O}(\mathbf{b}^2)$, and since most engineering flows have significant regions where $\mathcal{P} \geq \varepsilon$, we will replace the constant c_1 with the coefficient

$$-(C_1 + C_1^* \mathcal{P}/\varepsilon)$$

where C_1 and C_1^* are constants. This yields the following model for the pressure-strain correlation:

$$\begin{aligned} \Pi_{ij} \;=\; & -(C_1\varepsilon + C_1^*\mathcal{P})b_{ij} + C_2\varepsilon(b_{ik}b_{kj} \\ & -\frac{1}{3}b_{mn}b_{mn}\delta_{ij}) + (C_3 - C_3^* II^{\frac{1}{2}})K\overline{S}_{ij} \\ & +C_4K(b_{ik}\overline{S}_{jk} + b_{jk}\overline{S}_{ik} - \frac{2}{3}b_{mn}\overline{S}_{mn}\delta_{ij}) \\ & +C_5K(b_{ik}\overline{W}_{jk} + b_{jk}\overline{W}_{ik}). \end{aligned} \tag{62}$$

Although (62) is topologically equivalent to (58) in so far as the equilibrium states are concerned, it will give rise to different temporal evolutions. We feel that it is better to use (62) as our final model for the pressure-strain correlation since all terms that are of a comparable order in b_{ij} have been maintained for asymptotic consistency.

Before using constraints (ii) - (v) to calibrate the SSG model given by (62), a few comments are in order concerning the relationship between this new model and previously proposed models. The SSG model is not significantly more complicated than the commonly used Launder, Reece, and Rodi model which can be obtained from (62) in the linear limit as C_1^*, C_2 and C_3^* go to zero. In fact, the SSG model is substantially simpler than the recently proposed nonlinear models of Shih and Lumley (1985) and Fu, Launder, and Tselepidakis (1987) (see Appendix B).

The coefficients C_1 and C_2 have been calibrated by considering the return to isotropy problem (see Sarkar and Speziale 1989). Of course, for the return to isotropy problem, only the terms containing the coefficients C_1 and C_2 in the pressure-strain correlation survive (i.e., the rapid pressure-strain correlation vanishes). Based upon realizability, dynamical systems considerations, and the phase space portrait of return to isotropy experiments, the following values of C_1 and C_2 were arrived at by Sarkar and Speziale (1989):

$$C_1 = 3.4 \tag{63}$$

$$C_2 \equiv 3(C_1 - 2) = 4.2. \tag{64}$$

Interestingly enough, the value of $C_1 = 3.4$ is quite close to the value of 3.6 for the Rotta coefficient that is currently used in the basic model of Launder and his co-workers. However, as demonstrated by Sarkar and Speziale (1989), the quadratic term containing C_2 is crucial to properly capture the experimental trends. In Figure 1, the predictions of the SSG model and the Launder, Reece, and Rodi (LRR) model are compared in the $\xi - \eta$ phase space with the experimental data of Choi and Lumley (1984) for the return to isotropy from plane strain. The SSG model exhibits a curved trajectory that is well within the range of the experimental data; the LRR model – as well as any model for which $C_2 = 0$ – erroneously predicts a straight line trajectory. In Figures 2(a) - (b), the predictions of the SSG model and the LRR model for the temporal evolution of the anisotropy tensor are compared with experimental data for the relaxation from plane strain experiment of Choi and Lumley (1984) and plane contraction experiment of Le Penven, Gence, and Comte-Bellot (1985). The SSG model, on balance, yields improved predictions over the LRR model. For more detailed discussions and comparisons, the reader is referred to the paper by Sarkar and Speziale (1989) where this quadratic model for the slow pressure-strain correlation was compared with data from four independent experiments on the return to isotropy.

Constraint (ii), which requires consistency with RDT for a homogeneously strained turbulence that is initially isotropic, is commonly enforced in the turbulence modeling literature. While the dynamical systems analysis presented in Section 3 can guarantee proper long-time behavior, this RDT constraint can be of considerable assistance in ensuring proper short-time behavior; if a model properly captures both the short and long-time behavior, it stands an excellent chance of performing well for all times. This RDT result requires that (see Crow 1968)

$$\lim_{\mathbf{b} \to 0} \Pi_{ij} = \frac{4}{5} K \overline{S}_{ij} \tag{65}$$

and, hence, that

$$C_3 = \frac{4}{5} \tag{66}$$

for the SSG model. We found that models which deviated significantly from (66) performed poorly in homogeneous shear flows (e.g., such models yielded spurious points of inflection in the time evolution of the turbulent kinetic energy).

Constraints (iii) - (iv) were used to calibrate the remaining constants in the model, namely, C_1^*, C_3^*, C_4, and C_5 as well as the constant $C_{\epsilon 1}$ in the modeled ϵ-transport equation. This was done using a value of $C_{\epsilon 2} = 1.83$ (as opposed to the more commonly adopted value of 1.92) which yields a power law decay in isotropic turbulence with an exponent of 1.2 – a value which is in better agreement with available experimental data as discussed by

Reynolds (1987). It was not possible to obtain the exact equilibrium values of Tavoularis and Corrsin (1981) for homogeneous shear flow and satisfy the RDT results of Bertoglio for rotating shear flow (i.e., constraints (iii) - (iv)). A numerical optimization yielded the values of $C_1^* = 1.80, C_3^* = 1.30, C_4 = 1.25, C_5 = 0.40$ and $C_{\epsilon 1} = 1.44$ as the best compromise. The equilibrium values obtained from the SSG model (using these values of the constants) for homogeneous shear flow are compared with the values obtained from the Launder, Reece, and Rodi model and the experiments of Tavoularis and Corrsin (1981) in Table 1. From these results, it is clear that the predictions of the SSG model are well within the range of the experiments whereas the predictions of the Launder, Reece, and Rodi model deviate significantly. Furthermore, the SSG model predicts that the largest growth rate in rotating shear flow occurs when $\Omega/S \approx 0.22$ and that a flow restabilization occurs when $\Omega/S > 0.53$ in comparison to the corresponding RDT results of $\Omega/S = 0.25$ and $\Omega/S > 0.5$ (see Bertoglio 1982). These predictions of the SSG model are considerably better than those of the LRR model which erroneously predicts that the largest growth rate occurs when $\Omega/S = 0.14$ and that a flow restabilization occurs when $\Omega/S > 0.37$. A more detailed discussion of the performance of the models in rotating shear flow will be presented in the next section.

The SSG model has been carefully calibrated to perform well in shear flows both with and without added rotational strains. It is our belief that this will significantly enhance the performance of the model in turbulent boundary layers with streamline curvature – an analogous flow with a variety of important engineering applications. However, unlike other recently derived models for the pressure-strain correlation such as the Shih-Lumley (1985) model and the Fu, Launder, and Tselepidakis (1987) model, the SSG model given by equation (62) does not satisfy the strong form of realizability. The strong form of realizability (see Lumley 1978) constitutes a sufficient condition to guarantee positive component energies in homogeneous turbulent flows. The SSG model only satisfies a weak form of realizability wherein the turbulent kinetic energy is guaranteed to be positive; this is a direct consequence of the form of the modeled ε-transport equation (see Speziale 1989b). We decided to opt for the weaker form of realizability for two major reasons. First, if the turbulent kinetic energy is positive, realizability can only be violated by fairly large anisotropies, such that

$$\|\mathbf{b}\| > \frac{1}{3}$$

(where $\|\cdot\|$ is the L_2 norm or maximum eigenvalue) which are outside of the expected domain of applicability of such idealized models. It must be kept in mind that, so long as the model yields a positive turbulent kinetic energy, it can be applied to a flow (it is primarily negative kinetic energies that are computationally fatal). Second, it has been our experience that models which satisfy the strong form of realizability become computationally "stiff" in flows

with large anisotropies. This results from the fact that the finite difference form of the modeled equations usually do not exactly satisfy realizability (see Speziale and Mac Giolla Mhuiris 1989a). No such problems are encountered by the weak form of realizability since it is satisfied exactly by most standard numerical formulations of the model. Finally, it should be mentioned that the SSG model was not forced to satisfy material frame indifference (MFI) in the limit of two-dimensional turbulence (Speziale 1983) which constitutes another extreme constraint that is a rigorous consequence of the Navier-Stokes equations. It has recently become apparent to us that when such extreme constraints as MFI and strong realizability (correct as they may be for general flows) are applied to *highly idealized models*, there is a strong possibility that the model will become overly biased so that it performs poorly in the more commonly encountered turbulent flows.

5. PERFORMANCE OF THE SSG MODEL IN HOMOGENEOUS FLOWS

The SSG model given by equation (62) will now be tested in four independent homogeneous turbulent flows. For the purpose of clarity, we will summarize the values of the constants that were arrived at in the previous section:

$$C_1 = 3.4,\ C_1^* = 1.80,\ C_2 = 4.2 \tag{67}$$

$$C_3 = \frac{4}{5},\ C_3^* = 1.30,\ C_4 = 1.25 \tag{68}$$

$$C_5 = 0.40,\ C_{\varepsilon 1} = 1.44,\ C_{\varepsilon 2} = 1.83. \tag{69}$$

The problem of homogeneous turbulent shear flow in a rotating frame will be considered first. For this case, the mean velocity gradients and the rotation rate of the reference frame are given by

$$\frac{\partial \overline{v}_i}{\partial x_j} = \begin{pmatrix} 0 & S & 0 \\ 0 & 0 & 0 \\ 0 & 0 & 0 \end{pmatrix} \tag{70}$$

$$\Omega_i = (0, 0, \Omega), \tag{71}$$

respectively, in matrix form. The initial conditions correspond to a state of isotropic turbulence where

$$b_{ij} = 0,\ K = K_0,\ \varepsilon = \varepsilon_0 \tag{72}$$

at time $t = 0$. It was shown by Speziale and Mac Giolla Mhuiris (1989a) that the solution only depends on the initial conditions through the dimensionless parameter ε_0/SK_0; the dependence of the solution on the shear rate and rotation rate is exclusively through the dimensionless parameter Ω/S. Two types of equilibrium solutions have been established

for this problem (Speziale and Mac Giolla Mhuiris 1989a): one where $(\varepsilon/SK)_\infty = 0$ which exists for all Ω/S and one where $(\varepsilon/SK)_\infty > 0$ which exists only for a small intermediate band of values for Ω/S. The zero equilibrium value is associated predominantly with stable flow wherein K and ε undergo a power-law time decay; the nonzero equilibrium values are associated with unstable flow wherein K and ε undergo an exponential time growth. The two solutions undergo an exchange of stabilities for intermediate values of Ω/S (which includes the case of pure shear where $\Omega/S = 0$). In this fashion, the second-order closures are able to account for both the shear instability – with its exponential time growth of disturbance kinetic energy – and the stabilizing (or destabilizing) effect of rotations on shear flow.

In Figures 3(a) - (c), the predictions of the SSG model for the time evolution of turbulent kinetic energy are compared with those of the LRR model and the results of the large-eddy simulations of Bardina, Ferziger, and Reynolds (1983) for rotating shear flow. From these figures, it is clear that the SSG model does a much better overall job of capturing the trends of the large-eddy simulations. Several observations are noteworthy: (a) the LRR model exhibits too strong a growth rate for pure shear ($\Omega/S = 0$) in comparison to the SSG model and large-eddy simulations, (b) both the SSG and LRR models yield too weak a growth rate for the $\Omega/S = 0.25$ case, however, the SSG model is substantially better, and (c) the SSG model properly captures the weak growth rate that occurs for $\Omega/S = 0.5$, whereas the LRR model erroneously predicts a flow restabilization. The premature flow restabilization predicted by the LRR model at $\Omega/S \approx 0.37$ is somewhat serious since, in addition to the results of large-eddy simulations, linear stability theory and RDT predict that there should be unstable flow for the entire range of $0 \leq \Omega/S \leq 0.5$ (see Lezius and Johnston 1976 and Bertoglio 1982). As mentioned earlier, the SSG model does not predict a flow restabilization until $\Omega/S > 0.53$.

It would be useful at this point to compare the performance of the SSG model in rotating shear flow with that of some newer models that have been recently proposed. Three such models – the model of Shih and Lumley (1985), the model of Fu, Launder, and Tselepidakis (1987), and the RNG model of Yakhot and Orszag (1988) – were compared in a recent study of Speziale, Gatski, and Mac Giolla Mhuiris (1989). It was established in that study that the Fu, Launder, and Tselepidakis (FLT) model performed the best among these models in rotating shear flow. Hence, for simplicity, we will only compare the SSG model with the FLT model. In Figures 4(a) - (c), the results for the turbulent kinetic energy obtained from the SSG model and the FLT model for the rotation rates of $\Omega/S = 0, \Omega/S = 0.25$, and $\Omega/S = 0.50$ are compared with the large-eddy simulations of Bardina, Ferziger, and Reynolds (1983) for rotating shear flow. It is clear from these results that the SSG model properly captures the trends of the large-eddy simulations which indicate that all three cases

are unstable and that the $\Omega/S = 0.25$ case has the strongest growth rate. On the otherhand, the FLT model erroneously predicts that the $\Omega/S = 0$ and $\Omega/S = 0.25$ cases are equally energetic and that the $\Omega/S = 0.5$ case has undergone a restabilization. Comparable to the LRR model, the FLT model erroneously predicts a premature restabilization at $\Omega/S \approx 0.39$. It may be of concern that a heavy emphasis has been placed on comparisons with large-eddy simulations for rotating shear flow (unfortunately, no direct simulations or physical experiments have been conducted for this problem). However, it must be emphasized that the critical evaluations have been based on which states should be more energetic - results which have been confirmed independently by RDT and linear stability theory.

A bifurcation diagram for the general hierarchy of closure models (61) is shown in Figure 5 for rotating shear flow. Here, the equilibrium value of $(\varepsilon/SK)_\infty$ is plotted as a function of Ω/S. The SSG model as well as the other commonly used models have the same topological structure in rotating shear flow as indicated in Figure 5. There are two equilibrium solutions: the solution where $(\varepsilon/SK)_\infty = 0$ exists for all Ω/S but becomes unstable in the interval AB; the nonzero solution for $(\varepsilon/SK)_\infty$, which lies on the semi-ellipse ACB, exchanges stabilities with the trivial solution $(\varepsilon/SK)_\infty = 0$ in the interval $A < \Omega/S < B$. For $\Omega/S < A - \delta A$ and $\Omega/S > B + \delta B$ (where δA and δB represent a small increment that depends on the model) the trivial equilibrium value of $(\varepsilon/SK)_\infty = 0$ is associated with solutions where the kinetic energy undergoes a power law decay with time; for $A - \delta A \leq \Omega/S \leq B + \delta B$, this trivial solution is associated with solutions where the kinetic energy undergoes a power law growth with time. The nonzero equilibrium values $(\varepsilon/SK)_\infty > 0$ (on the semi-ellipse ACB) are associated with solutions where the kinetic energy grows exponentially with time. It can be shown (see Speziale and Mac Giolla Mhuiris 1989a) that the growth rate λ for $A < \Omega/S < B$ is given by

$$\lambda = (\alpha - 1)\left(\frac{\varepsilon}{SK}\right)_\infty \tag{73}$$

where $\alpha = (C_{\varepsilon 2} - 1)/(C_{\varepsilon 1} - 1)$. Hence, point C - which corresponds to the maximum value of $(\varepsilon/SK)_\infty$ - represents the most energetic state with the largest growth rate of kinetic energy.

The coordinates $[\Omega/S, (\varepsilon/SK)_\infty]$ of points A, B, and C (in Figure 5) for the Launder, Reece, and Rodi model and the SSG model are given below:

LRR Model

$$A = [-0.09, 0],\ B = [0.37, 0],\ C = [0.14, 0.167]$$

SSG Model

$$A = [-0.09, 0],\ B = [0.53, 0],\ C = [0.22, 0.254].$$

The improved performance of the SSG model in rotating shear flow is largely due to the fact that its most energetic state (point C on the bifurcation diagram shown in Figure 5) is located in close proximity to $\Omega/S = 0.25$ - the value predicted by rapid distortion theory. However, it needs to be mentioned at this point that the reason we were not able to satisfy this RDT result exactly is due to a defect in the general hierarchy of models (61). Due to (73) and the fact that the bifurcation diagram is symmetric about its most energetic state (point C in Figure 5), the general hierarchy of models (61) erroneously predicts Richardson number similarity if point C is located at $\Omega/S = 0.25$. Such models will yield solutions for K and ε that scale with the Richardson number

$$\mathrm{Ri} = -2(\Omega/S)(1 - 2\Omega/S) \tag{74}$$

and, thus, erroneously predict that the $\Omega/S = 0$ and $\Omega/S = 0.5$ cases are identical. Large-eddy simulations, RDT (Bertoglio 1982), and independent mathematical analyses of the Navier-Stokes equations (Speziale and Mac Giolla Mhuiris 1989b) indicate that the $\Omega/S = 0$ and $\Omega/S = 0.5$ cases are distinct. By moving the most energetic state a small distance to the left of $\Omega/S = 0.25$ - as is done with the SSG model - the proper growth rates obtained from large-eddy simulations for $\Omega/S = 0$ and $\Omega/S = 0.5$ can be reproduced (see Figures 3(a) and 3(c)). However, the substantially larger growth rate for $\Omega/S = 0.25$ shown in Figure 3(b) (which has independent support in the RDT calculations of Bertoglio 1982), cannot be reproduced by the SSG model. This is a defect in the general hierarchy of models (61) that is intimately tied to their prediction of universal equilibrium values for $II_\infty, III_\infty, (b_{33})_\infty$ and $(\mathcal{P}/\varepsilon)_\infty$ in plane homogeneous turbulent flows - an oversimplification that is not supported by physical or numerical experiments.[†] Nonetheless, despite this deficiency, the SSG model performs reasonably well - and is superior to other existing second-order closures - for rotating shear flow as evidenced by Table 1, Figures 3(a) - (c), and Figures 4(a) - (c).

Now, we will examine the performance of the SSG model in homogeneous plane strain turbulence for which the mean velocity gradients are given by

$$\frac{\partial \overline{v}_i}{\partial x_j} = \begin{pmatrix} S & 0 & 0 \\ 0 & -S & 0 \\ 0 & 0 & 0 \end{pmatrix} \tag{75}$$

and the turbulence evolves from an initial state of isotropy. Comparisons of the model predictions will be made with the direct numerical simulations of Lee and Reynolds (1985) on plane strain. Such comparisons must be made with caution due to the low turbulence Reynolds numbers of the direct simulations. However, comparisons with physical experiments (e.g.,

[†]It is not possible to tie this deficiency to the modeled ε-transport equation since all dependence on ε can be eliminated in the RDT limit.

Tucker and Reynolds 1968 and Gence and Mathieu 1980) are equally problematical due to the uncertainty in the initial conditions for ε/SK and possible large-scale contamination from the walls of the test apparatus.

In Figure 6, the time evolution of the turbulent kinetic energy for the LRR model and SSG model are compared with the direct simulations of Lee and Reynolds (1985) for plane strain corresponding to the initial condition $\varepsilon_0/SK_0 = 2.0$. It is clear from this figure that both models perform extremely well. In Figure 7, the time evolution of the non-zero components of the anisotropy tensor are shown. Although the quantitative accuracy of the models is not extremely good, it is clear that the SSG model does better than the LRR model and reproduces the crucial trends of the direct simulations. In Figures 8 - 9, the time evolution of the turbulent kinetic energy and non-zero components of the anisotropy tensor are shown corresponding to the initial condition of $\varepsilon_0/SK_0 = 1.0$. The same conclusions can be drawn from these results: the SSG model yields improved predictions over the LRR model and, on balance, compares reasonably well with the direct simulations which would be expected to have somewhat elevated anisotropies due to the lower turbulence Reynolds number. We will not make more extensive comparisons with the predictions of other turbulence models since our main purpose here was to simply establish that the alterations made in the LRR model – to yield the SSG model with its improved behavior in rotating shear flows – do not compromise its performance in plane strain.

Finally, we will examine the performance of the SSG model for the axisymmetric contraction and expansion in homogeneous turbulence. Since the SSG model (like virtually all other existing models for the pressure-strain correlation) was calibrated based on plane homogeneous turbulent flows, it would be desirable to assess its performance in a three-dimensional flow. For the axisymmetric contraction, the mean velocity gradients are given by

$$\frac{\partial \overline{v}_i}{\partial x_j} = \begin{pmatrix} S & 0 & 0 \\ 0 & -\frac{1}{2}S & 0 \\ 0 & 0 & -\frac{1}{2}S \end{pmatrix} \tag{76}$$

whereas in the axisymmetric expansion they take the form

$$\frac{\partial \overline{v}_i}{\partial x_j} = \begin{pmatrix} -S & 0 & 0 \\ 0 & \frac{1}{2}S & 0 \\ 0 & 0 & \frac{1}{2}S \end{pmatrix}. \tag{77}$$

The time evolution of each of these turbulent flows – from an initially isotropic state – will be considered. Hence, as with plane shear and plane strain, the solutions will only depend on the initial conditions through the parameter ε_0/SK_0. Comparisons will be made with the predictions of the LRR model and the direct numerical simulations of Lee and Reynolds (1985) for the same reasons as cited above.

In Figure 10, the time evolution of the turbulent kinetic energy for the axisymmetric contraction is shown corresponding to the initial condition $\varepsilon_0/SK_0 = 0.179$ which was taken from the direct simulations of Lee and Reynolds (1985). From these results, it is clear that the SSG model yields noticeably improved predictions over the LRR model; however, both models predict growth rates that are smaller than those in the direct simulations. In Figure 11, the time evolution of the nonzero components of the anisotropy tensor are shown for the axisymmetric contraction where $\varepsilon_0/SK_0 = 0.179$. While the differences between the SSG and LRR models is small, it is clear that the SSG model yields results that are more in line with the direct simulations.

In Figure 12, the time evolution of the turbulent kinetic energy for the axisymmetric expansion is shown for the initial condition $\varepsilon_0/SK_0 = 2.45$ taken from the direct numerical simulations of Lee and Reynolds (1985). It is clear from this figure that both the SSG and LRR models yield results that are in excellent agreement with the direct simulations. However, the time evolution of the nonzero components of the anisotropy tensor shown in Figure 13 show more significant differences. Here, the predictions of the SSG model appear to be substantially better than those of the LRR model.

6. CONCLUSIONS

The modeling of the pressure-strain correlation of turbulence has been considered based on invariance arguments and a dynamical systems approach. Several important conclusions have been drawn about the standard hierarchy of closures (61) which led to the development of a new model – the SSG model. A summary of these findings can be given as follows:

(i) It was proven that the standard hierarchy of models yields non-trivial values for the equilibrium states $II_\infty, III_\infty, (b_{33})_\infty$, and $(\mathcal{P}/\varepsilon)_\infty$ that are *universal* (i.e., that do not depend on ω/S, Ω/S or the initial conditions) for plane homogeneous turbulent flows. As a direct consequence of these universal invariants, it was shown that, for plane homogeneous turbulent flows, the general model (61) for the pressure-strain correlation is topologically equivalent to a substantially simpler model – the SSG model – which is only quadratically nonlinear in the anisotropy tensor.

(ii) The SSG model was calibrated by using existing data from isotropic decay experiments, return to isotropy experiments, and homogeneous shear flow experiments along with the RDT results of Crow (1968) and Bertoglio (1982). By means of this more systematic method of calibration, the SSG model was demonstrated to perform better than the Launder, Reece, and Rodi model – as well as the newer models of Shih and Lumley

and Fu, Launder, and Tselepidakis – for a variety of homogeneous turbulent flows. The flows that were examined included the challenging test case of rotating shear flow (where rotations can either stabilize or destabilize the flow) and the axisymmetric expansion/contraction which constitutes a three-dimensional mean turbulent flow.

(iii) Although the SSG model performs reasonably well for a variety of homogeneous turbulent flows, there are still major deficiencies with it that are intrinsic to this general hierarchy of models. These deficiencies, emanate from the prediction of universal equilibrium values for $II_\infty, III_\infty, (b_{33})_\infty$ and $(\mathcal{P}/\varepsilon)_\infty$ in plane homogeneous turbulent flows – an obvious oversimplification that is not supported by physical experiments. As a result of this deficiency, the general model (61) erroneously predicts that rotating shear flow has growth rates that are symmetric about their most energetic value. Hence, in order to satisfy the RDT constraint of Bertoglio (1982) – which puts the most energetic state at $\Omega/S = 0.25$ – the models must exhibit Richardson number similarity. This is inconsistent with the Navier-Stokes equations as proven by Speziale and Mac Giolla Mhuiris (1989b) and illustrated by Bardina, Ferziger, and Reynolds (1983).

(iv) Since the general model (61) for the pressure-strain correlation gives an incomplete picture of plane homogeneous turbulent flows no matter what form is taken for $\mathcal{A}_{ij}(\mathbf{b})$ and $\mathcal{M}_{ijk\ell}(\mathbf{b})$, we feel that the process of adding highly complex nonlinear terms in b_{ij} is somewhat questionable. Such complex nonlinear terms in the rapid pressure-strain correlation have been largely motivated by the desire to satisfy the strong form of realizability. However, it must be remembered that the strong form of this constraint only constitutes a sufficient condition for the satisfaction of realizability in homogeneous turbulent flows. Due to the relatively simple topological structure of the general model in rotating shear flow – which is in no way altered by the addition of more complex nonlinearities in b_{ij} – the application of the strong form of realizability either removes the degrees of freedom necessary to properly calibrate the model or leads to stiff behavior.

Despite the deficiencies discussed above, the SSG model seems to perform moderately well in a variety of homogeneous turbulent flows as documented in this paper. While further improvements would be most welcome, we feel that it is unlikely that they will come from the standard hierarchy of models (61). Fundamentally new approaches will be needed. Future research will be directed on two fronts. The SSG model will be implemented in a full second-order closure for the computation of a variety of complex aerodynamic flows that are of technological interest. We believe that when the SSG model is used within the framework

of a sound second-order closure, it may be possible to obtain acceptable engineering answers for a range of turbulent shear flows with streamline curvature. In parallel with this effort, entirely new directions in modeling the pressure-strain correlation will be pursued. These will involve the introduction of a tensor length scale – to better account for anisotropies – and the possible solution of a transport equation for $M_{ijk\ell}$ to account for history effects in the rapid pressure-strain. A closer examination of these issues will be the subject of a future paper.

ACKNOWLEDGEMENT

The authors would like to thank Dr. Nessan Mac Giolla Mhuiris for some helpful comments on the dynamical systems aspects of this paper.

References

Bardina, J., Ferziger, J. H., and Reynolds, W. C. 1983 Improved turbulence models based on large-eddy simulation of homogeneous, incompressible turbulent flows. *Stanford University Technical Report TF-19.*

Bertoglio, J. P. 1982 Homogeneous turbulent field within a rotating frame. *AIAA J.* **20**, 1175.

Choi, K. S. and Lumley, J. L. 1984 Return to isotropy of homogeneous turbulence revisited. *Turbulence and Chaotic Phenomena in Fluids* (T. Tatsumi, ed.), p. 267, North Holland.

Crow, S. C. 1968 Viscoelastic properties of fine-grained incompressible turbulence. *J. Fluid Mech.* **41**, 81.

Fu, S., Launder, B. E., and Tselepidakis, D. P. 1987 Accommodating the effects of high strain rates in modelling the pressure-strain correlation. UMIST *Mechanical Engineering Department Report* TFD/87/5.

Gence, J. N. and Mathieu, J. 1980 The return to isotropy of a homogeneous turbulence having been submitted to two successive plane strains. *J. Fluid Mech.* **101**, 555.

Hanjalic, K. and Launder, B. E. 1972 A Reynolds stress model of turbulence and its application to thin shear flows. *J. Fluid Mech.* **52**, 609.

Haworth, D. C. and Pope, S. B. 1986 A generalized Langevin model for turbulent flows. *Phys. Fluids* **29**, 387.

Launder, B. E., Reece, G., and Rodi, W. 1975 Progress in the development of a Reynolds stress turbulence closure. *J. Fluid Mech.*, **68**, 537.

Launder, B. E., Tselepidakis, D. P., and Younis, B. A. 1987 A second-moment closure study of rotating channel flow. *J. Fluid Mech.* **183**, 63.

Lee, M. J. and Reynolds, W. C. 1985 Numerical experiments on the structure of homogeneous turbulence. *Stanford University Technical Report TF-24.*

Le Penven, L., Gence, J. N., and Comte-Bellot, G. 1985 On the approach to isotropy of homogeneous turbulence: Effect of the partition of kinetic energy among the velocity components. *Frontiers in Fluid Mechanics* (S. H. Davis and J. L. Lumley, eds.), p. 1, Springer-Verlag.

Lezius, D. K. and Johnston, J. P. 1976 Roll-cell instabilities in rotating laminar and turbulent channel flow. *J. Fluid Mech.* **77**, 153.

Lumley, J. L. 1978 Turbulence modeling. *Adv. Appl. Mech.* **18**, 123.

Mellor, G. L. and Herring, H. J. 1973 A survey of mean turbulent field closure models. *AIAA J.* **11**, 590.

Reynolds, W. C. 1987 Fundamentals of turbulence for turbulence modeling and simulation. *Lecture Notes for Von Karman Institute, AGARD Lecture Series No. 86*, North Atlantic Treaty Organization.

Reynolds, W. C. 1988 *Private Communication.*

Rotta, J. C. 1951 Statistische Theorie Nichthomogener Turbulenz. *Z. Phys.* **129**, 547.

Rotta, J. C. 1972 Recent attempts to develop a generally applicable calculation method for turbulent shear flow layers. AGARD-CP-93, North Atlantic Treaty Organization.

Sarkar, S. and Speziale, C. G. 1989 A simple nonlinear model for the return to isotropy in turbulence. *Phys. Fluids A* (in press).

Shih, T-H. and Lumley, J. L. 1985 Modeling of pressure correlation terms in Reynolds stress and scalar flux equations. *Technical Report No. FDA-85-3*, Cornell University.

Smith, G. F. 1971 On isotropic functions of symmetric tensors, skew-symmetric tensors and vectors. *Int. J. Engng. Sci.* **9**, 899.

Speziale, C. G. 1983 Closure models for rotating two-dimensional turbulence. *Geophys. & Astrophys. Fluid Dynamics* **23**, 69.

Speziale, C. G. 1987 Second-order closure models for rotating turbulent flows. *Quart. Appl. Math.* **45**, 721.

Speziale, C. G. 1989a Turbulence modeling in non-inertial frames of reference. *Theoret. & Comput. Fluid Dynamics* **1**, 3.

Speziale, C. G. 1989b Discussion of turbulence modeling: Past and future. *Lecture Notes in Physics* (in press).

Speziale, C. G., Gatski, T. B., and Mac Giolla Mhuiris, N. 1989 A critical comparison of turbulence models for homogeneous shear flows in a rotating frame. *Proceedings of the Seventh Symposium on Turbulent Shear Flows*, Vol. 2, p. 27.3.1, Stanford University Press.

Speziale, C. G. and Mac Giolla Mhuiris, N. 1989a On the prediction of equilibrium states in homogeneous turbulence. *J. Fluid Mech.* **209**, 591.

Speziale, C. G. and Mac Giolla Mhuiris, N. 1989b Scaling laws for homogeneous turbulent shear flows in a rotating frame. *Phys. Fluids A* **1**, 294.

Tavoularis, S. and Corrsin, S. 1981 Experiments in nearly homogeneous turbulent shear flows with a uniform mean temperature gradient. Part I. *J. Fluid Mech.* **104**, 311.

Tucker, H. J. and Reynolds, A. J. 1968 The distortion of turbulence by irrotational plane strain. *J. Fluid Mech.* **32**, 657.

Weinstock, J. 1981 Theory of the pressure-strain rate correlation for Reynolds stress turbulence closures. Part 1. *J. Fluid Mech.* **105**, 369.

Weinstock, J. 1982 Theory of the pressure-strain rate. Part 2. *J. Fluid Mech.* **116**, 1.

Yakhot, V. and Orszag, S. A. 1988 *Private Communication.*

APPENDIX A

Consider the tensor function

$$F_{ij} = F_{ij}(\mathbf{b}, \overline{\mathbf{S}}', \overline{\omega}'). \tag{A1}$$

Form invariance under coordinate transformations (28) requires that F_{ij} be of the form (see Smith 1971):

$$\begin{aligned}
\mathbf{F} \;=\; & \alpha_0\mathbf{I} + \alpha_1\mathbf{b} + \alpha_2\mathbf{b}^2 + \alpha_3\overline{\mathbf{S}}' + \alpha_4\overline{\mathbf{S}}'^2 \\
& + \alpha_5(\mathbf{b}\overline{\mathbf{S}}' + \overline{\mathbf{S}}'\mathbf{b}) + \alpha_6(\mathbf{b}^2\overline{\mathbf{S}}' + \overline{\mathbf{S}}'\mathbf{b}^2) \\
& + \alpha_7(\mathbf{b}\overline{\mathbf{S}}'^2 + \overline{\mathbf{S}}'^2\mathbf{b}) + \alpha_8(\mathbf{b}^2\overline{\mathbf{S}}'^2 + \overline{\mathbf{S}}'^2\mathbf{b}^2) \\
& + \alpha_9(\mathbf{b}\overline{\omega}' - \overline{\omega}'\mathbf{b}) + \alpha_{10}\overline{\omega}'\mathbf{b}\overline{\omega}' \\
& + \alpha_{11}(\mathbf{b}^2\overline{\omega}' - \overline{\omega}'\mathbf{b}^2) + \alpha_{12}(\overline{\omega}'\mathbf{b}\overline{\omega}'^2 - \overline{\omega}'^2\mathbf{b}\overline{\omega}') \\
& + \alpha_{13}(\overline{\mathbf{S}}'\overline{\omega}' - \overline{\omega}'\overline{\mathbf{S}}') + \alpha_{14}\overline{\omega}'\overline{\mathbf{S}}'\overline{\omega}' \\
& + \alpha_{15}(\overline{\mathbf{S}}'^2\overline{\omega}' - \overline{\omega}'\overline{\mathbf{S}}'^2) + \alpha_{16}(\overline{\omega}'\overline{\mathbf{S}}'\overline{\omega}'^2 - \overline{\omega}'^2\overline{\mathbf{S}}'\overline{\omega}') + \alpha_{17}\overline{\omega}'^2
\end{aligned} \tag{A2}$$

where α_i depend on all possible invariants, i.e.,

$$\begin{aligned}
\alpha_i \;=\; & \alpha_i(II, III, tr\ \overline{\omega}'^2, tr\ \overline{\mathbf{S}}'^2, tr\ \overline{\mathbf{S}}'^3, tr\ \mathbf{b}\overline{\mathbf{S}}', tr\ \mathbf{b}^2\overline{\mathbf{S}}', \\
& tr\ \mathbf{b}\overline{\mathbf{S}}'^2, tr\ \mathbf{b}^2\overline{\mathbf{S}}'^2, tr\ \mathbf{b}\overline{\omega}'^2, tr\ \mathbf{b}^2\overline{\omega}'^2, tr\ \overline{\omega}'\mathbf{b}\overline{\omega}'^2, \\
& tr\ \overline{\mathbf{S}}'\overline{\omega}'^2, tr\ \overline{\mathbf{S}}'^2\overline{\omega}'^2, tr\ \overline{\omega}'\overline{\mathbf{S}}'\overline{\omega}'^2, tr\ \mathbf{b}\overline{\mathbf{S}}'\overline{\omega}', tr\ \mathbf{b}^2\overline{\mathbf{S}}'\overline{\omega}', \\
& tr\ \mathbf{b}\overline{\omega}'^2\overline{\mathbf{S}}', tr\ \mathbf{b}\overline{\mathbf{S}}'^2\overline{\omega}'), \qquad i = 0, 1, 2, \ldots, 17.
\end{aligned} \tag{A3}$$

Taking the linear part of F_{ij} in $\overline{S}'_{ij}$ and $\overline{\omega}'_{ij}$ yields the equation

$$\begin{aligned}
\mathbf{F}^{(L)} \;=\; & \beta_0\mathbf{I} + \beta_1\mathbf{b} + \beta_2\mathbf{b}^2 + \beta_3\overline{\mathbf{S}}' + \beta_4(\mathbf{b}\overline{\mathbf{S}}' \\
& + \overline{\mathbf{S}}'\mathbf{b}) + \beta_5(\mathbf{b}^2\overline{\mathbf{S}}' + \overline{\mathbf{S}}'\mathbf{b}^2) \\
& + \beta_6(\mathbf{b}\overline{\omega}' - \overline{\omega}'\mathbf{b}) + \beta_7(\mathbf{b}^2\overline{\omega}' - \overline{\omega}'\mathbf{b}^2)
\end{aligned} \tag{A4}$$

where

$$\beta_0 = \beta_{00}(II, III) + \beta_{01}(II, III)tr(\mathbf{b}\cdot\overline{\mathbf{S}}') + \beta_{02}(II, III)tr(\mathbf{b}^2\cdot\overline{\mathbf{S}}') \tag{A5}$$

$$\beta_1 = \beta_{10}(II, III) + \beta_{11}(II, III)tr(\mathbf{b}\cdot\overline{\mathbf{S}}') + \beta_{12}(II, III)tr(\mathbf{b}^2\cdot\overline{\mathbf{S}}') \tag{A6}$$

$$\beta_2 = \beta_{20}(II, III) + \beta_{21}(II, III)tr(\mathbf{b} \cdot \overline{\mathbf{S}}') + \beta_{22}(II, III)tr(\mathbf{b}^2 \cdot \overline{\mathbf{S}}') \qquad (A7)$$

$$\beta_i = \beta_i(II, III), \quad i = 3, 4, \cdots, 7. \qquad (A8)$$

Then, by taking the deviatoric part of $F_{ij}^{(L)}$ (since Π_{ij} is traceless) and multiplying by ε we obtain Π_{ij}:

$$\Pi_{ij} = \varepsilon(F_{ij}^{(L)} - \frac{1}{3}F_{kk}^{(L)}\delta_{ij}). \qquad (A9)$$

Equation (29) results when (A4) - (A8) are substituted into (A9) and the identities in equation (27) are made use of.

APPENDIX B

The pressure-strain models of Shih and Lumley (1985) and Fu, Launder, and Tselepidakis (1987) take the following form:

Shih-Lumley Model

$$
\begin{aligned}
\Pi_{ij} \;=\; & -\beta\varepsilon b_{ij} + \left(\frac{4}{5} + 8\alpha_5\right) K\overline{S}_{ij} \\
& -\frac{2}{3}(1-\alpha_5)\left[\tau_{ik}\left(\frac{\partial \overline{v}_j}{\partial x_k} + e_{mkj}\Omega_m\right)\right. \\
& \left. +\tau_{jk}\left(\frac{\partial \overline{v}_i}{\partial x_k} + e_{mki}\Omega_m\right) - \frac{2}{3}\tau_{mn}\overline{S}_{mn}\delta_{ij}\right] \\
& +\left(\frac{2}{3} + \frac{16}{3}\alpha_5\right)\left[\tau_{ik}\left(\frac{\partial \overline{v}_k}{\partial x_j} + e_{mjk}\Omega_m\right)\right. \\
& \left. +\tau_{jk}\left(\frac{\partial \overline{v}_k}{\partial x_i} + e_{mik}\Omega_m\right) - \frac{2}{3}\tau_{mn}\overline{S}_{mn}\delta_{ij}\right] \\
& +\frac{6}{5}\tau_{mn}\overline{S}_{mn}b_{ij} + \frac{4}{15}[\tau_{ik}\overline{W}_{jk} + \tau_{jk}\overline{W}_{ik}] \\
& +\frac{1}{5K}\left\{\left[\tau_{ik}\left(\frac{\partial \overline{v}_j}{\partial x_\ell} + e_{m\ell j}\Omega_m\right)\right.\right. \\
& \left.\left. +\tau_{jk}\left(\frac{\partial \overline{v}_i}{\partial x_\ell} + e_{m\ell i}\Omega_m\right)\right]\tau_{k\ell} - 2\tau_{i\ell}\tau_{jm}\overline{S}_{\ell m}\right\}
\end{aligned}
\tag{B1}
$$

where

$$\alpha_5 = -\frac{1}{10}(1 + 0.8\sqrt{F}), \quad F = 1 + 9II + 27III \tag{B2}$$

$$II = -\frac{1}{2}b_{ij}b_{ij}, \quad III = \frac{1}{3}b_{ij}b_{jk}b_{ki} \tag{B3}$$

$$\beta = 2 + \frac{1}{9}F\{80.1\ell n[1 + 62.4(-II + 2.3III)]\} \tag{B4}$$

Fu, Launder, and Tselepidakis Model

$$
\begin{aligned}
\Pi_{ij} \;=\; & -C_1^*\varepsilon\sqrt{F}\left[2b_{ij}+4\gamma\left(b_{ik}b_{kj}-\frac{1}{3}b_{mn}b_{mn}\delta_{ij}\right)\right] \\
& -0.6\left[\tau_{ik}\left(\frac{\partial\overline{v}_j}{\partial x_k}+e_{mkj}\Omega_m\right)\right. \\
& \left.+\tau_{jk}\left(\frac{\partial\overline{v}_i}{\partial x_k}+e_{mki}\Omega_m\right)-\frac{2}{3}\tau_{mn}\frac{\partial\overline{v}_m}{\partial x_n}\delta_{ij}\right] \\
& +1.2\tau_{mn}\frac{\partial\overline{v}_m}{\partial x_n}b_{ij}-\frac{1}{5K}\left\{2\tau_{kj}\tau_{\ell i}\overline{S}_{k\ell}\right. \\
& \left.-\tau_{\ell k}\left[\tau_{ik}\left(\frac{\partial\overline{v}_j}{\partial x_\ell}+e_{m\ell j}\Omega_m\right)+\tau_{jk}\left(\frac{\partial\overline{v}_i}{\partial x_\ell}+e_{m\ell i}\Omega_m\right)\right]\right\} \\
& +r\{16II(\tau_{ik}\overline{W}_{jk}+\tau_{jk}\overline{W}_{ik}) \\
& -24b_{mi}b_{nj}(\tau_{mk}\overline{W}_{nk}+\tau_{nk}\overline{W}_{mk})\}
\end{aligned}
\tag{B5}
$$

where

$$
C_1^* = -60II, \quad \gamma = 0.6, \quad r = 0.7. \tag{B6}
$$

LIST OF FIGURES

Figure 12. Time evolution of the turbulent kinetic energy in the axisymmetric expansion for $\varepsilon_0/SK_0 = 2.45$. Comparison of the predictions of the LRR model and SSG model with the direct simulations of Lee and Reynolds (1985).

Figure 13. Time evolution of the anisotropy tensor in the axisymmetric expansion for $\varepsilon_0/SK_0 = 2.45$. Comparison of the predictions of the LRR model and SSG model with the direct simulations of Lee and Reynolds (1985).

Equilibrium Values	LRR Model	SSG Model	Experiments
$(b_{11})_\infty$	0.193	0.204	0.201
$(b_{22})_\infty$	-0.096	-0.148	-0.147
$(b_{12})_\infty$	-0.185	-0.156	-0.150
$(SK/\epsilon)_\infty$	5.65	5.98	6.08

Table 1. Comparison of the predictions of the Launder, Reece and Rodi (LRR) model and the Speziale, Sarkar and Gatski (SSG) model with the experiments of Tavoularis and Corrsin (1981) on homogeneous turbulent shear flow.

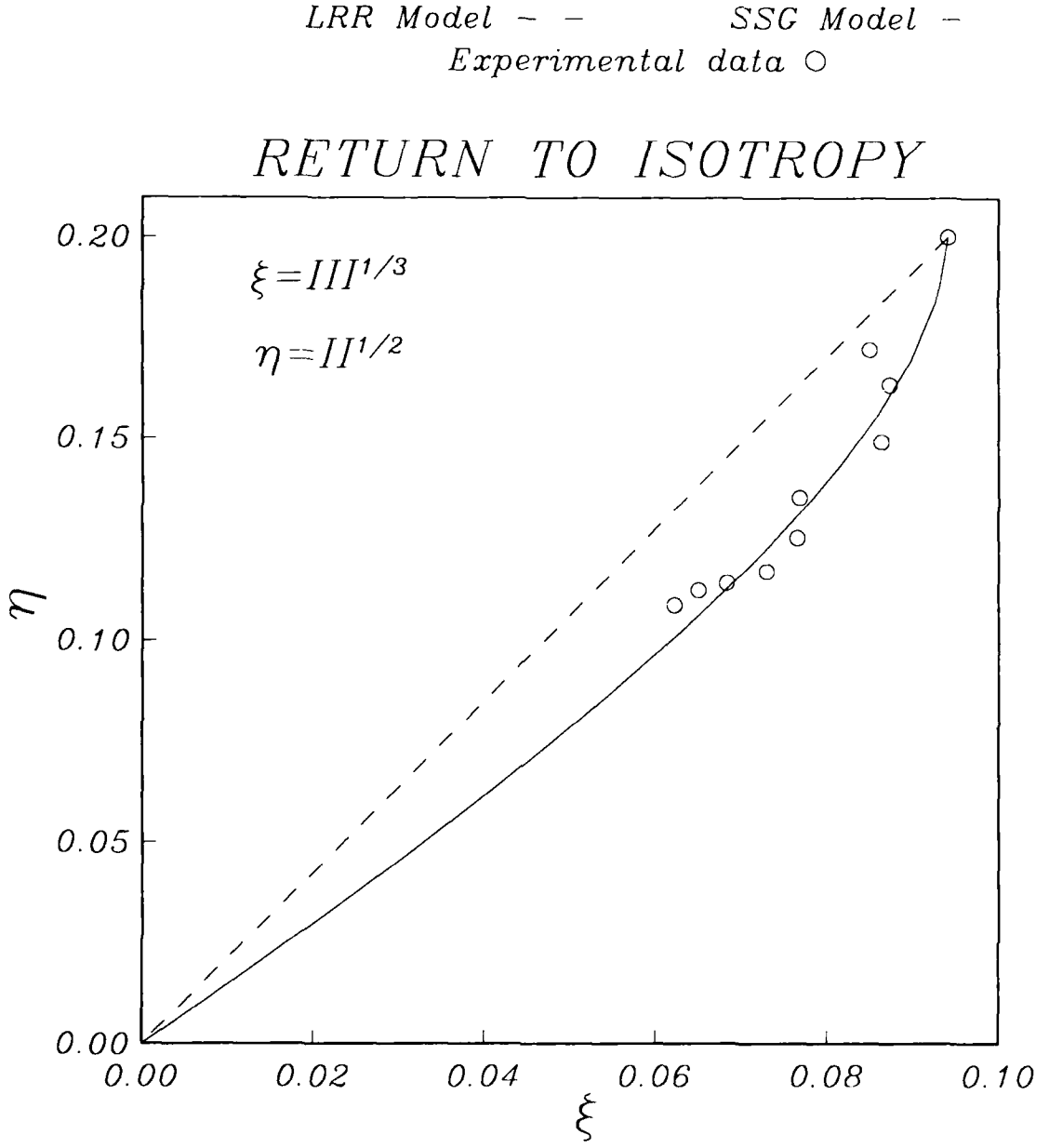

Figure 1. Phase space of the return to isotropy problem: Comparison of the predictions of the SSG model and LRR model with the plane strain experiment of Choi and Lumley (1984).

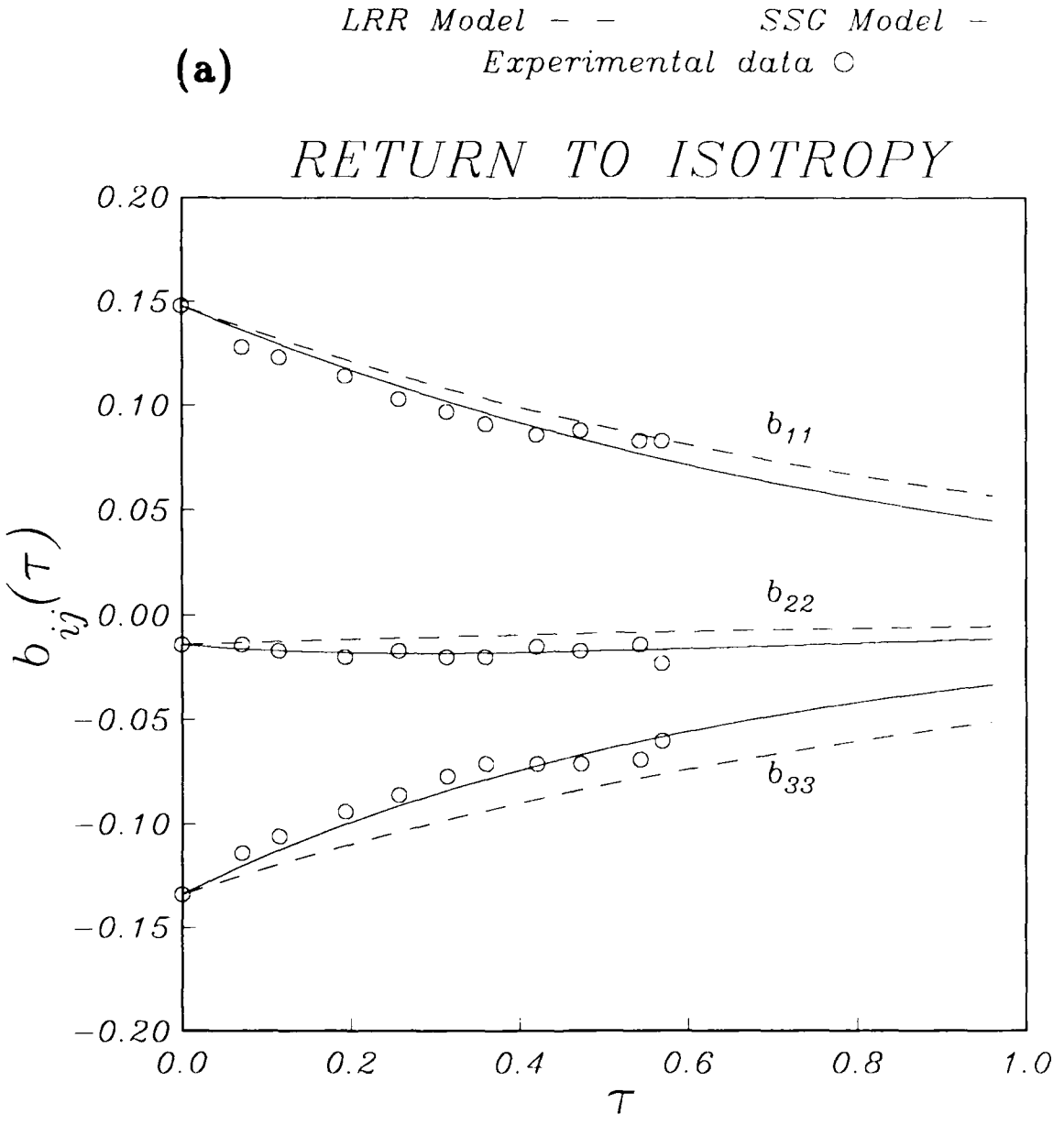

Figure 2. Time evolution of the anisotropy tensor during the return to isotropy. Comparison of the predictions of the SSG model and LRR model with experiments: (a) the plane strain experiment of Choi and Lumley (1984), and (b) the plane contraction experiment of Le Penven, Gence, and Comte-Bellot (1985).

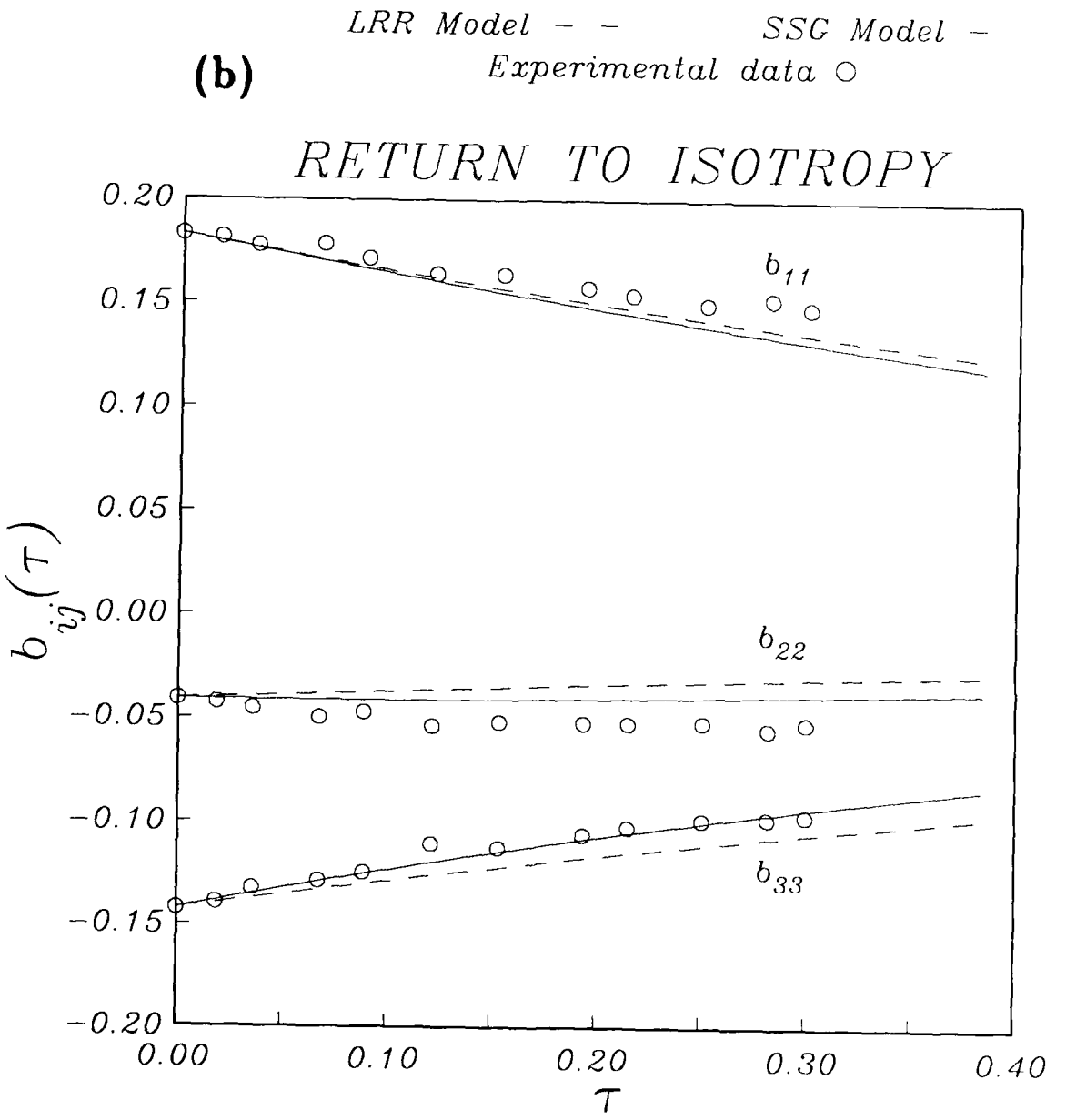

Figure 2. Time evolution of the anisotropy tensor during the return to isotropy. Comparison of the predictions of the SSG model and LRR model with experiments: (a) the plane strain experiment of Choi and Lumley (1984), and (b) the plane contraction experiment of Le Penven, Gence, and Comte-Bellot (1985).

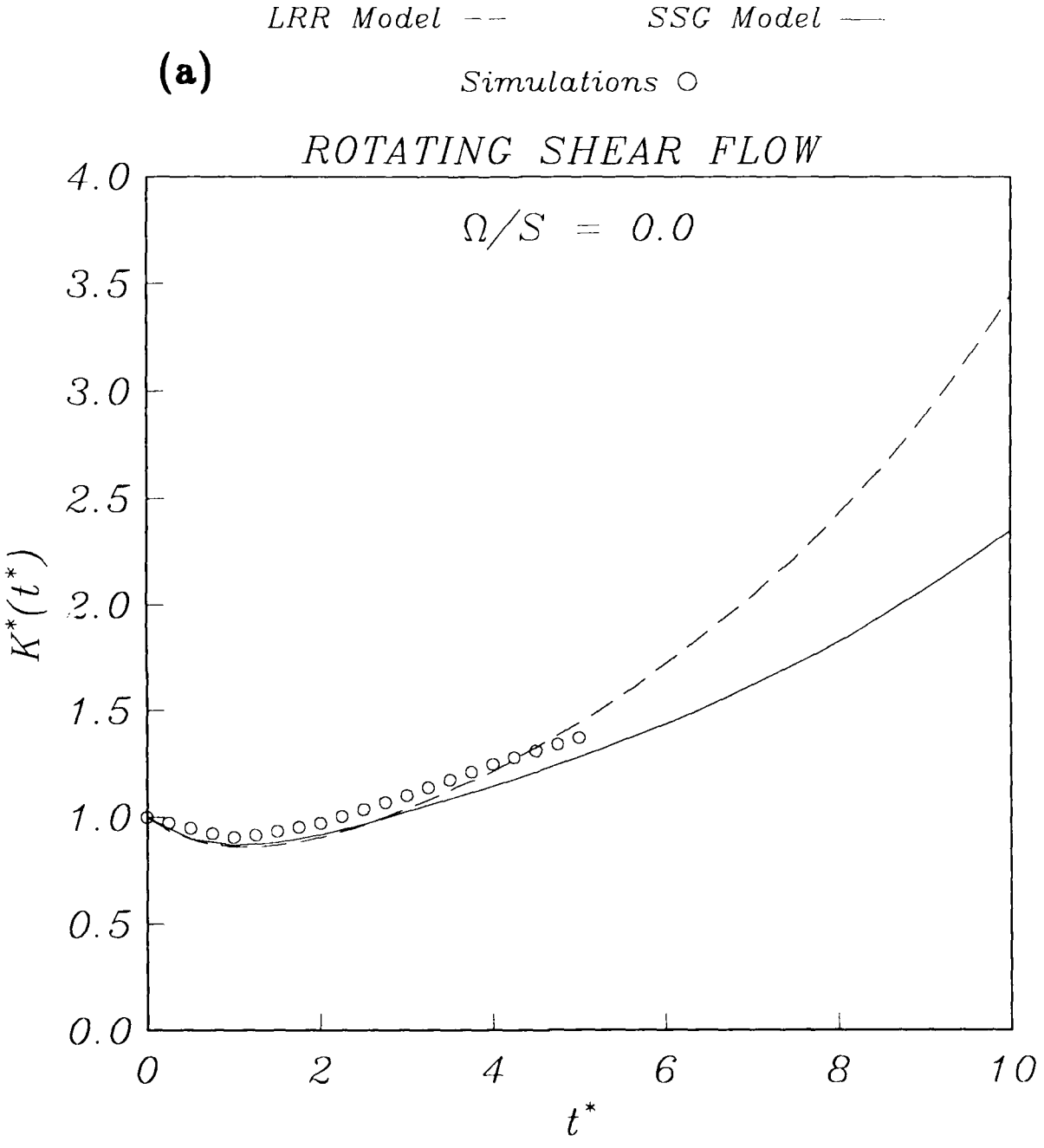

Figure 3. Time evolution of the turbulent kinetic energy in rotating shear flows. Comparison of the predictions of the SSG model and LRR model with the large-eddy simulation of Bardina, Ferziger, and Reynolds (1983) for $\varepsilon_0/SK_0 = 0.296$: (a) $\Omega/S = 0$, (b) $\Omega/S = 0.25$, and (c) $\Omega/S = 0.5$.

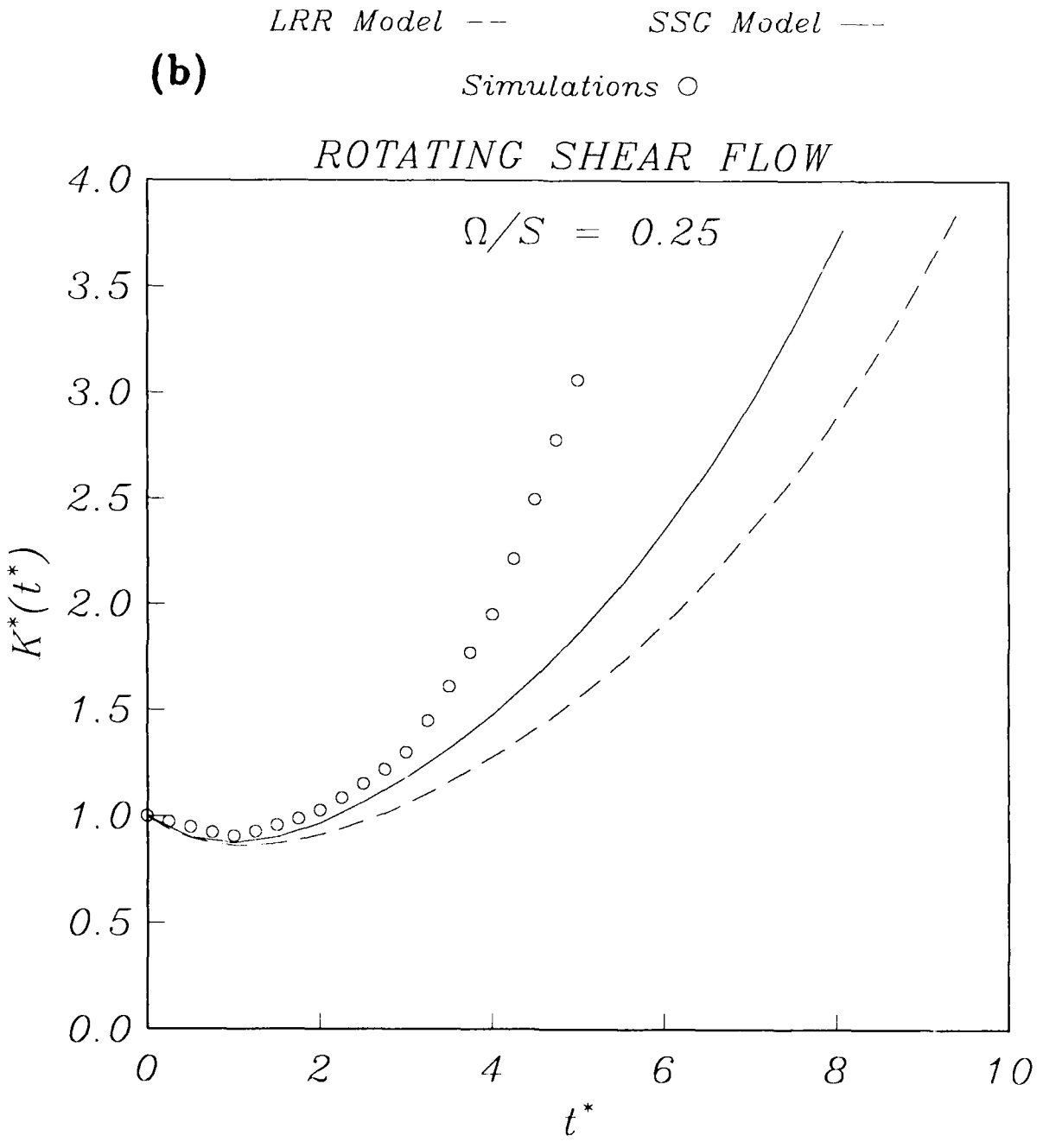

Figure 3. Time evolution of the turbulent kinetic energy in rotating shear flows. Comparison of the predictions of the SSG model and LRR model with the large-eddy simulation of Bardina, Ferziger, and Reynolds (1983) for $\varepsilon_0/SK_0 = 0.296$: (a) $\Omega/S = 0$, (b) $\Omega/S = 0.25$, and (c) $\Omega/S = 0.5$.

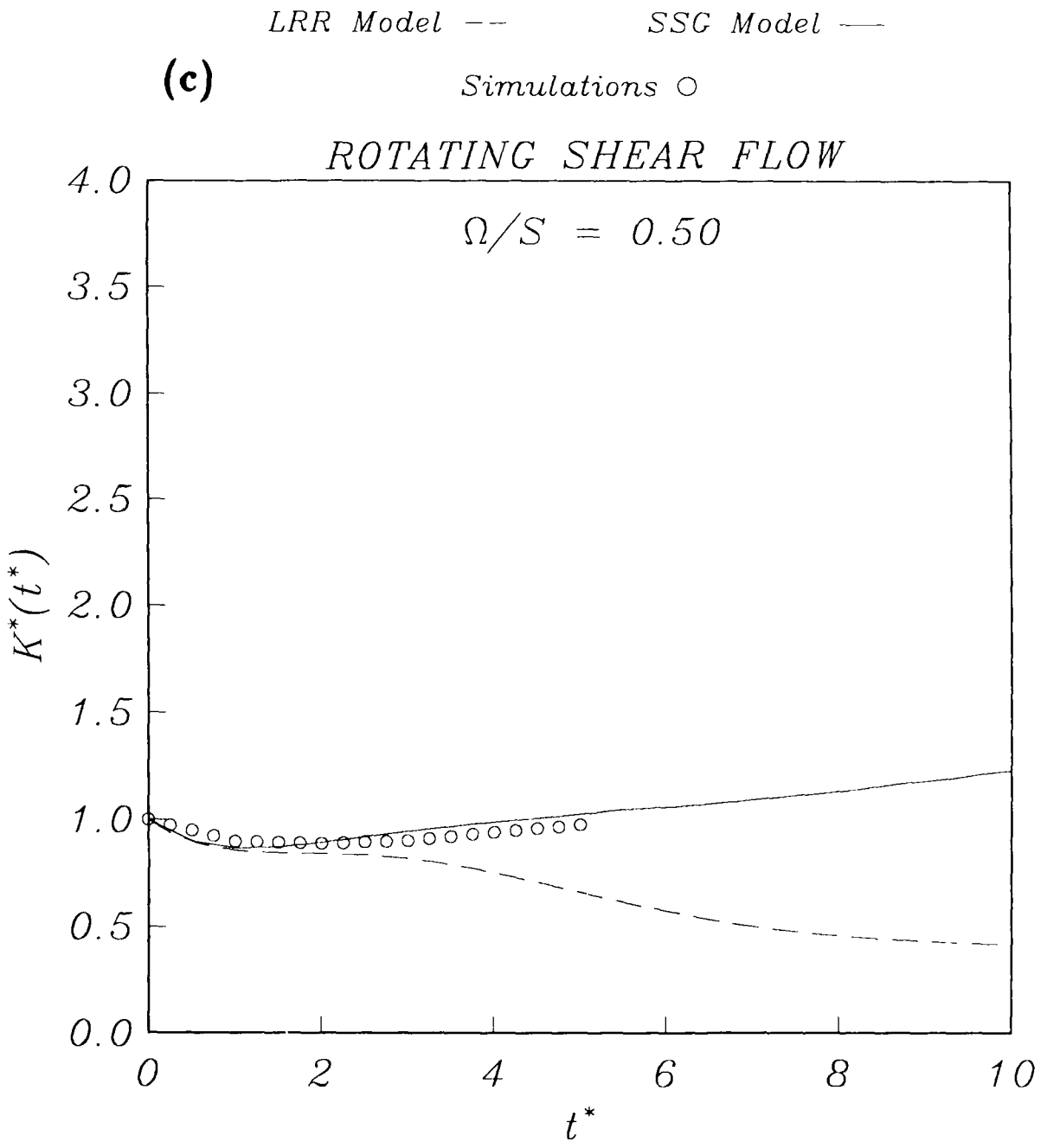

Figure 3. Time evolution of the turbulent kinetic energy in rotating shear flows. Comparison of the predictions of the SSG model and LRR model with the large-eddy simulation of Bardina, Ferziger, and Reynolds (1983) for $\varepsilon_0/SK_0 = 0.296$: (a) $\Omega/S = 0$, (b) $\Omega/S = 0.25$, and (c) $\Omega/S = 0.5$.

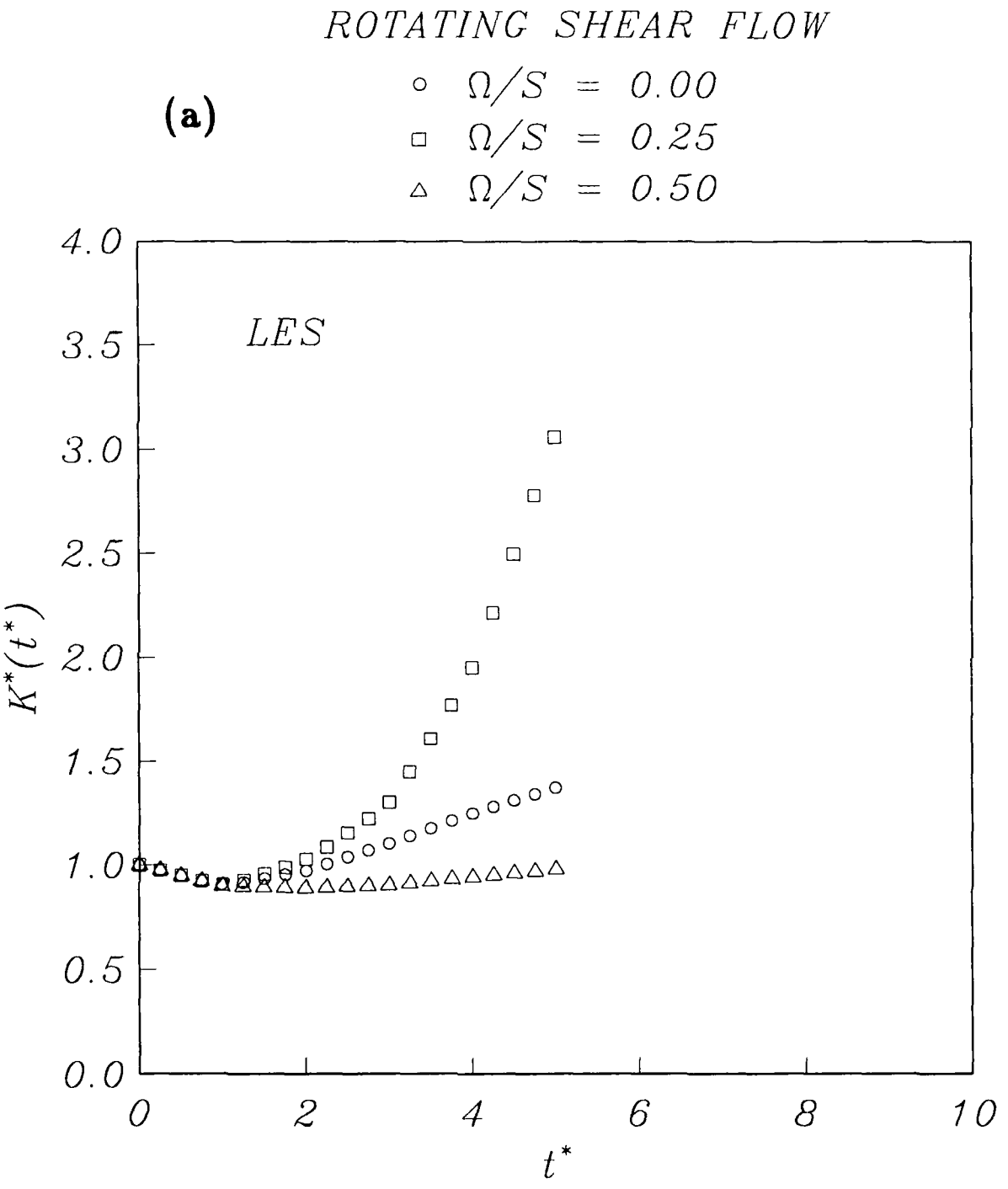

Figure 4. Comparison of the models with large-eddy simulations (LES) of rotating shear flow for $\Omega/S = 0, 0.25$ and 0.5: (a) LES of Bardina, Ferziger, and Reynolds (1983), (b) FLT model, and (c) SSG model.

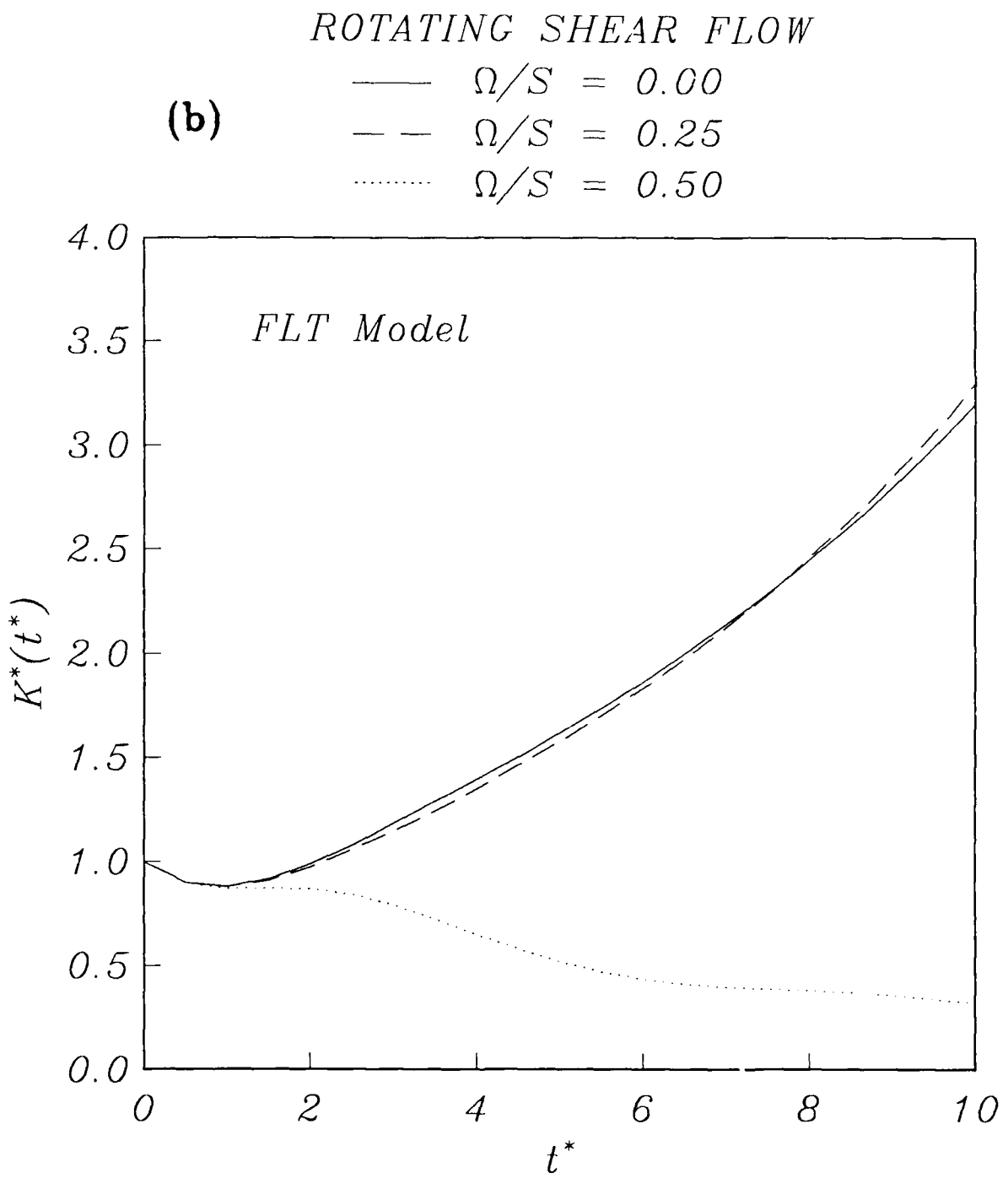

Figure 4. Comparison of the models with large-eddy simulations (LES) of rotating shear flow for $\Omega/S = 0, 0.25$ and 0.5: (a) LES of Bardina, Ferziger, and Reynolds (1983), (b) FLT model, and (c) SSG model.

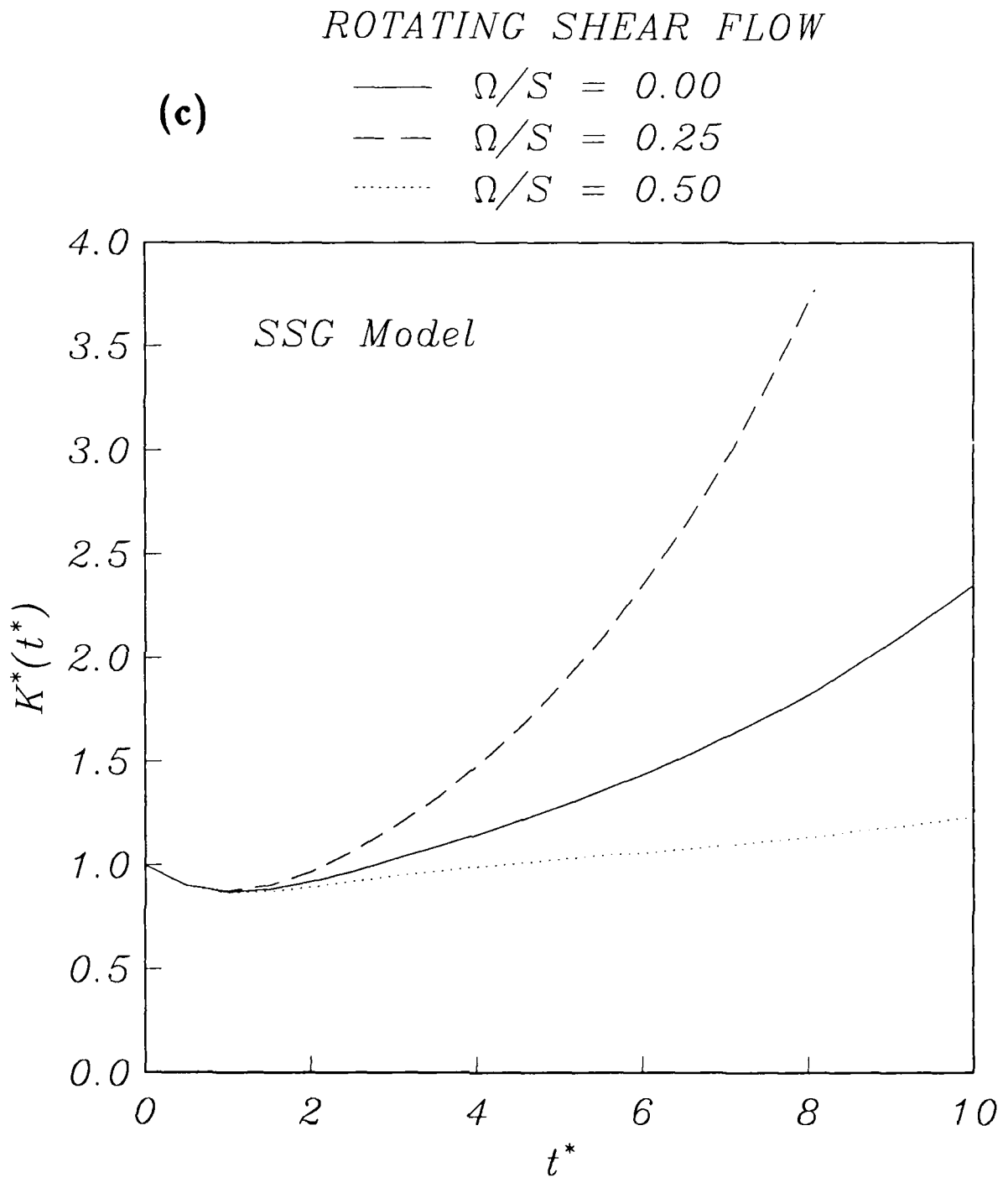

Figure 4. Comparison of the models with large-eddy simulations (LES) of rotating shear flow for $\Omega/S = 0, 0.25$ and 0.5: (a) LES of Bardina, Ferziger, and Reynolds (1983), (b) FLT model, and (c) SSG model.

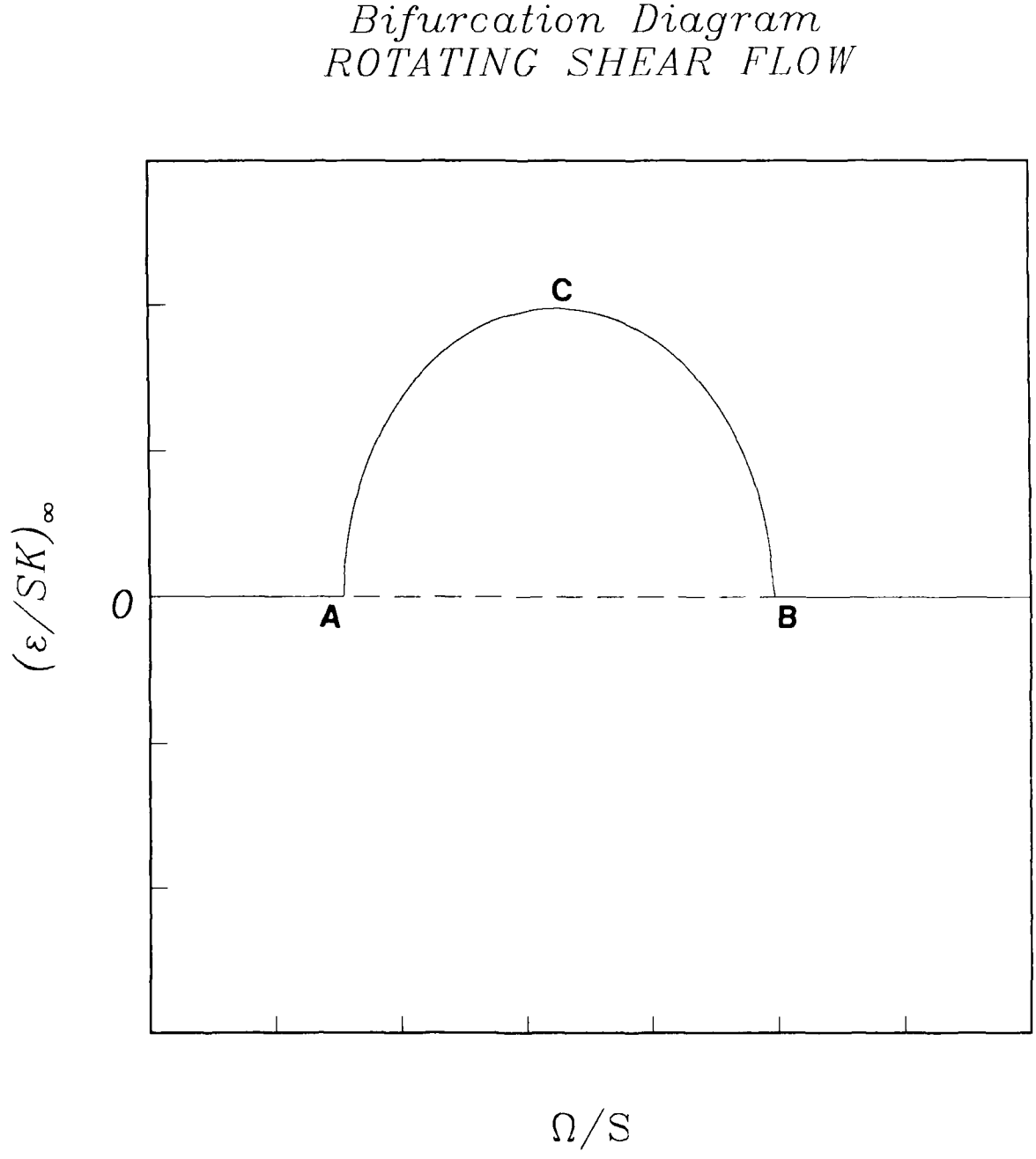

Figure 5. Bifurcation diagram for rotating shear flow.

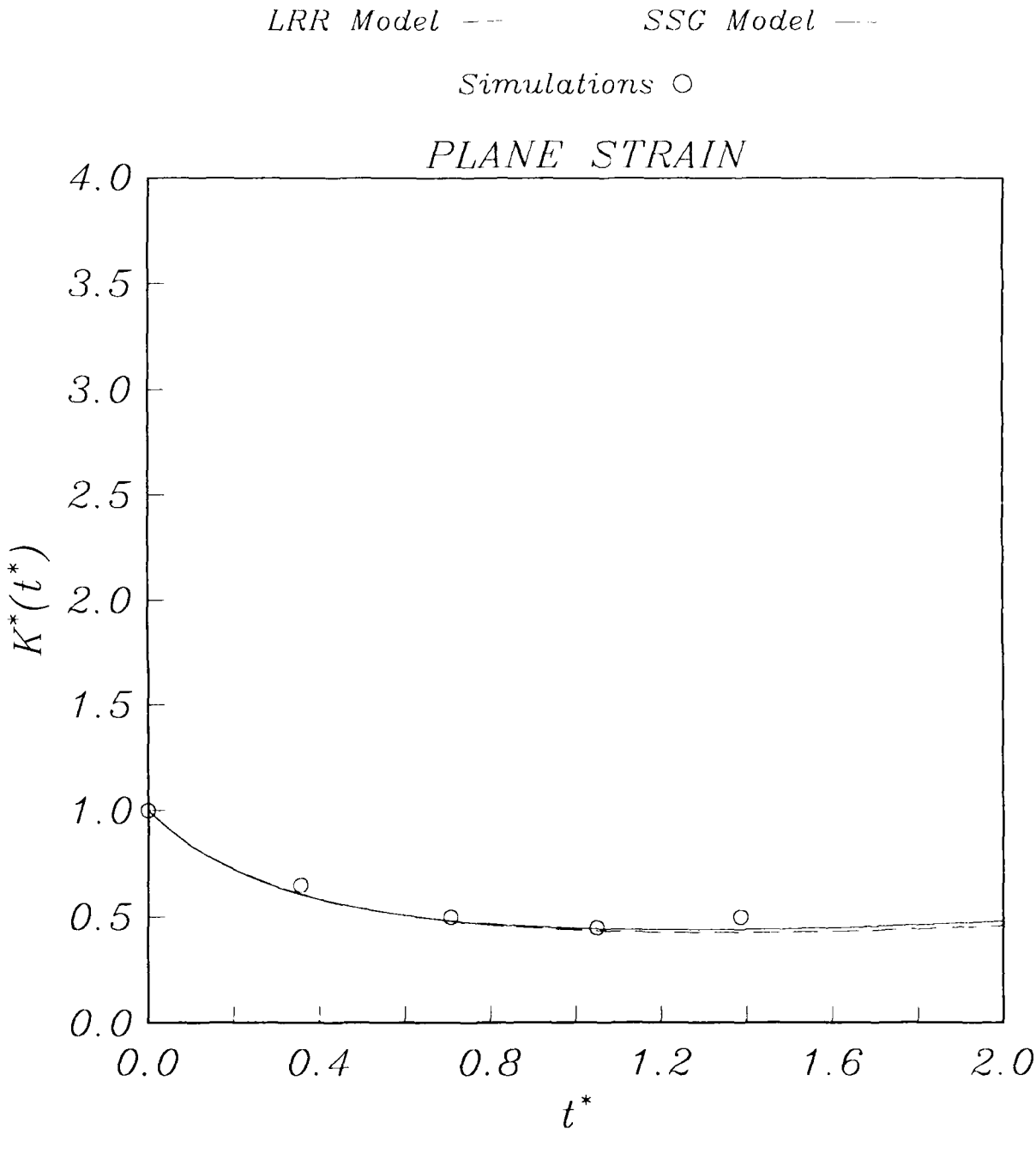

Figure 6. Time evolution of the turbulent kinetic energy in plane strain for $\varepsilon_0/SK_0 = 2.0$. Comparison of the predictions of the LRR model and SSG model with the direct simulations of Lee and Reynolds (1985).

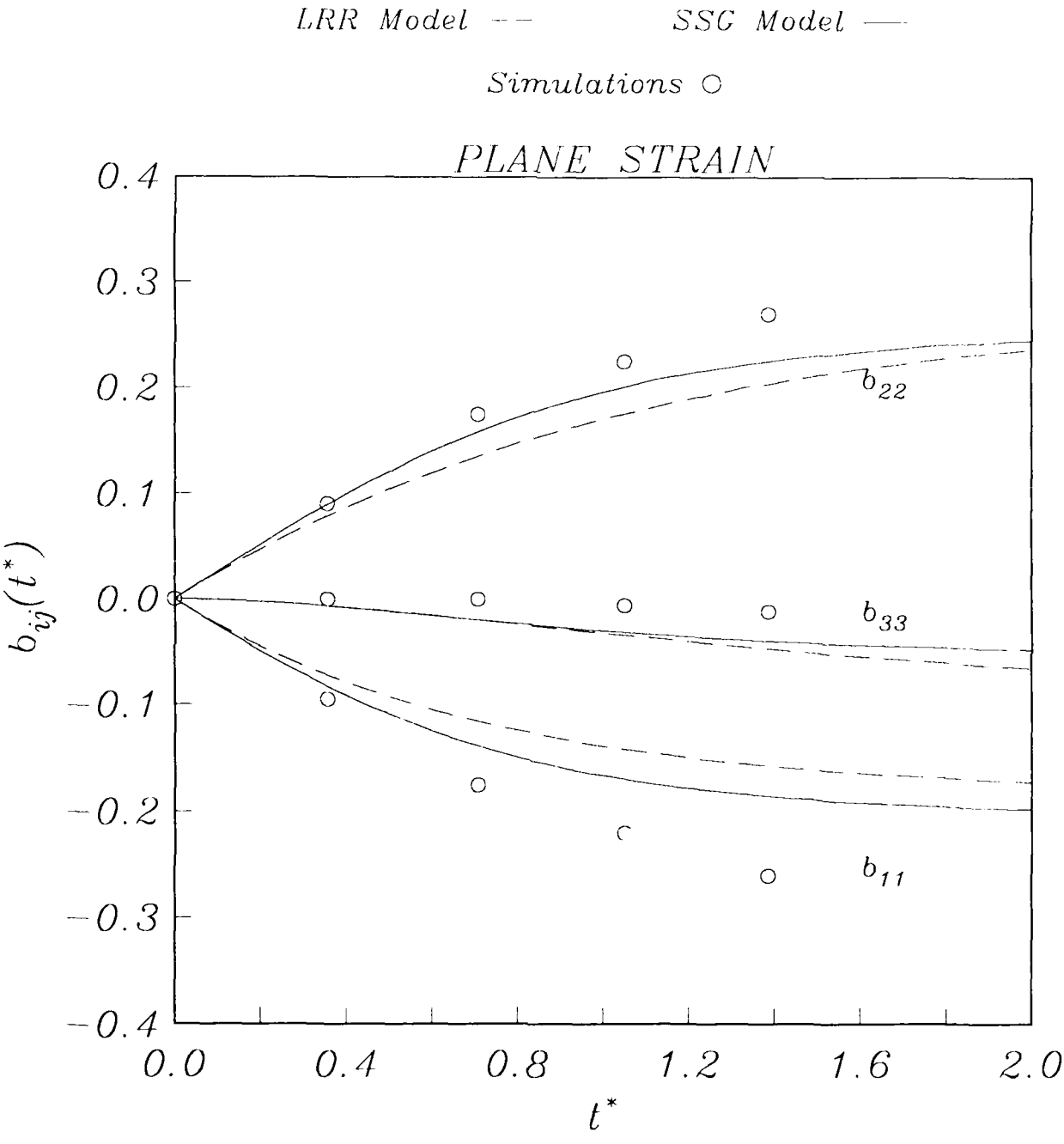

Figure 7. Time evolution of the anisotropy tensor in plane strain for $\varepsilon_0/SK_0 = 2.0$. Comparison of the predictions of the LRR model and SSG model with the direct simulations of Lee and Reynolds (1985).

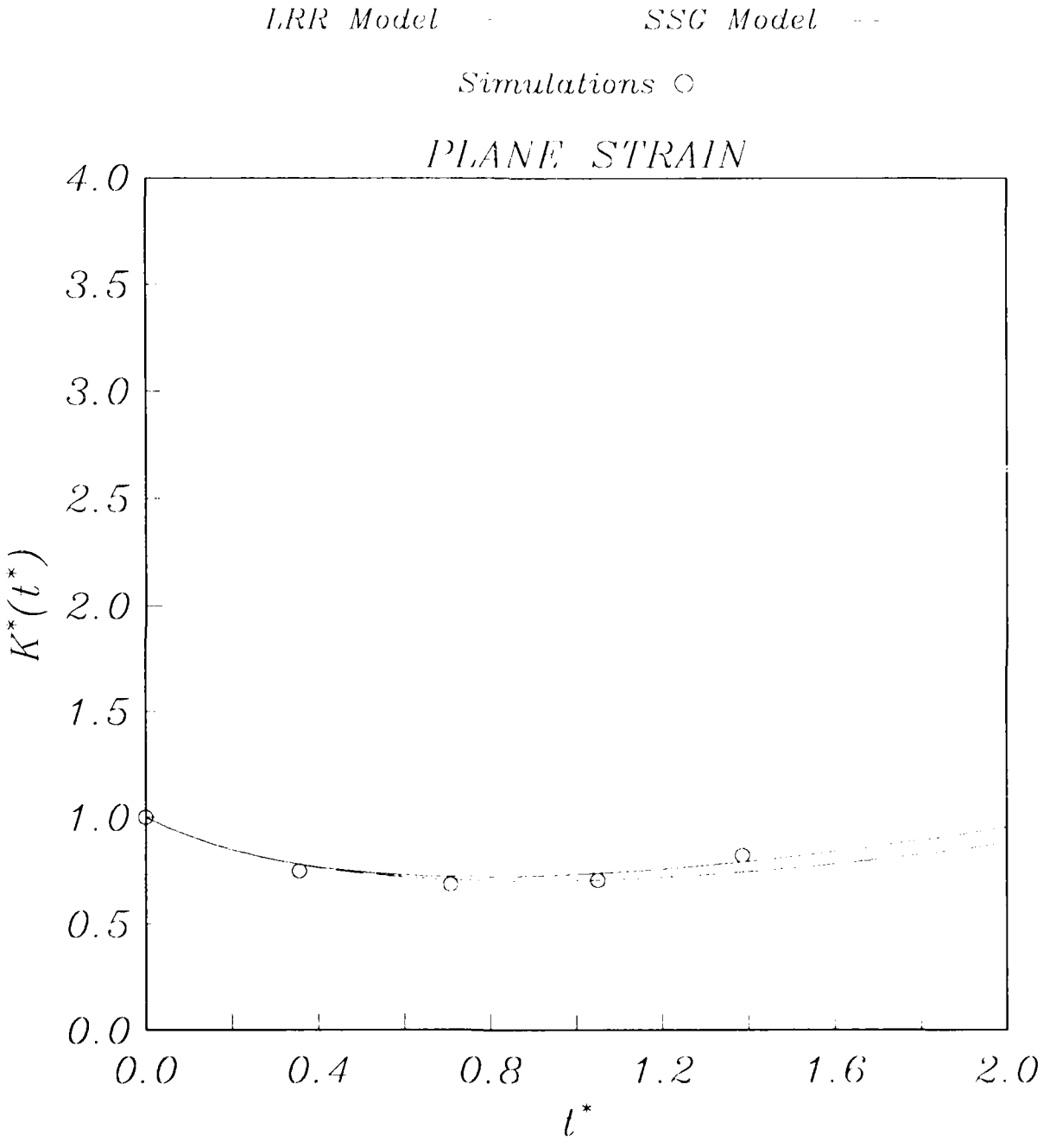

Figure 8. Time evolution of the turbulent kinetic energy in plane strain for $\varepsilon_0/SK_0 = 1.0$. Comparison of the predictions of the LRR model and SSG model with the direct simulations of Lee and Reynolds (1985).

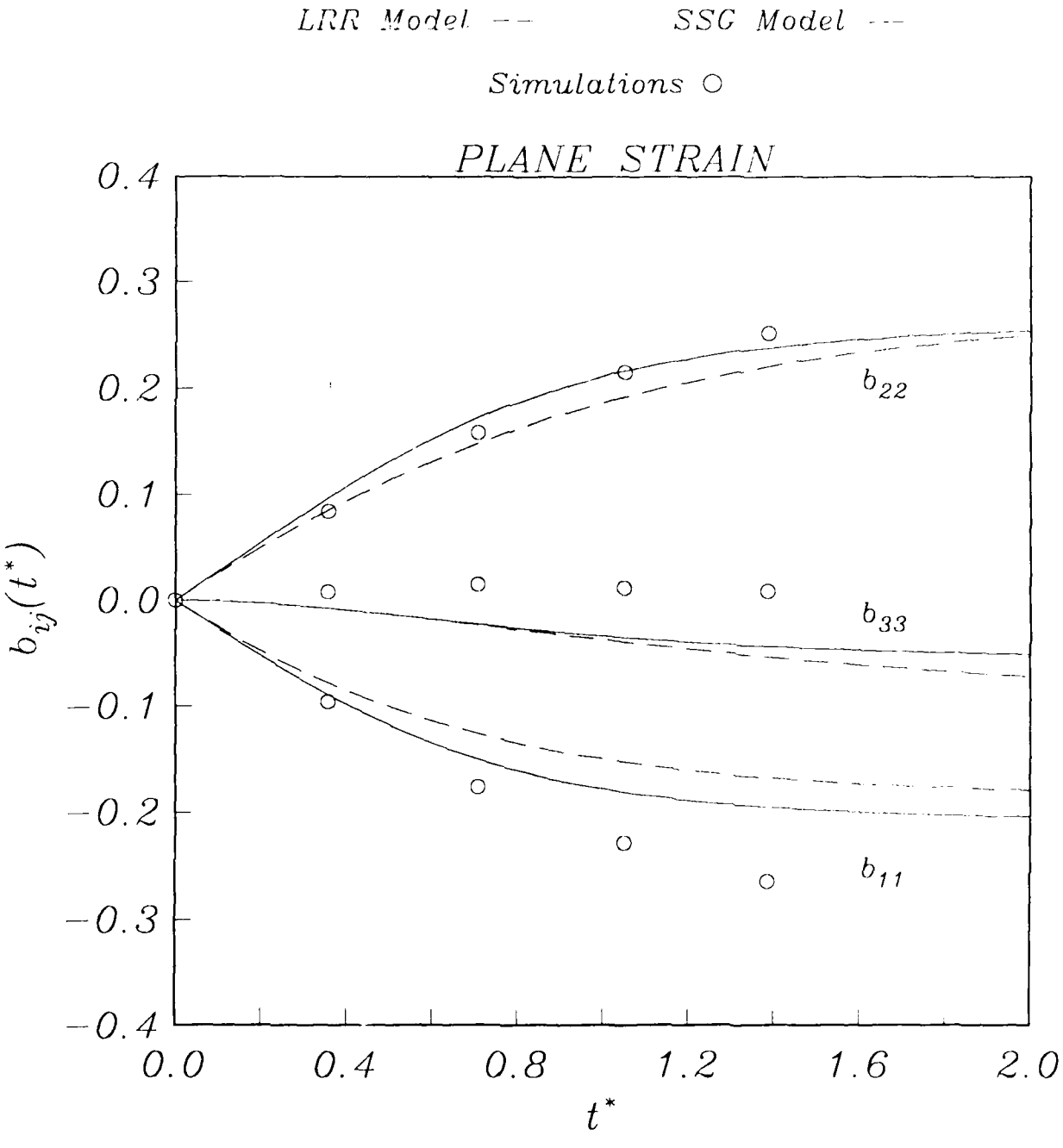

Figure 9. Time evolution of the anisotropy tensor in plane strain for $\epsilon_0/SK_0 = 1.0$. Comparison of the predictions of the LRR model and SSG model with the direct simulations of Lee and Reynolds (1985).

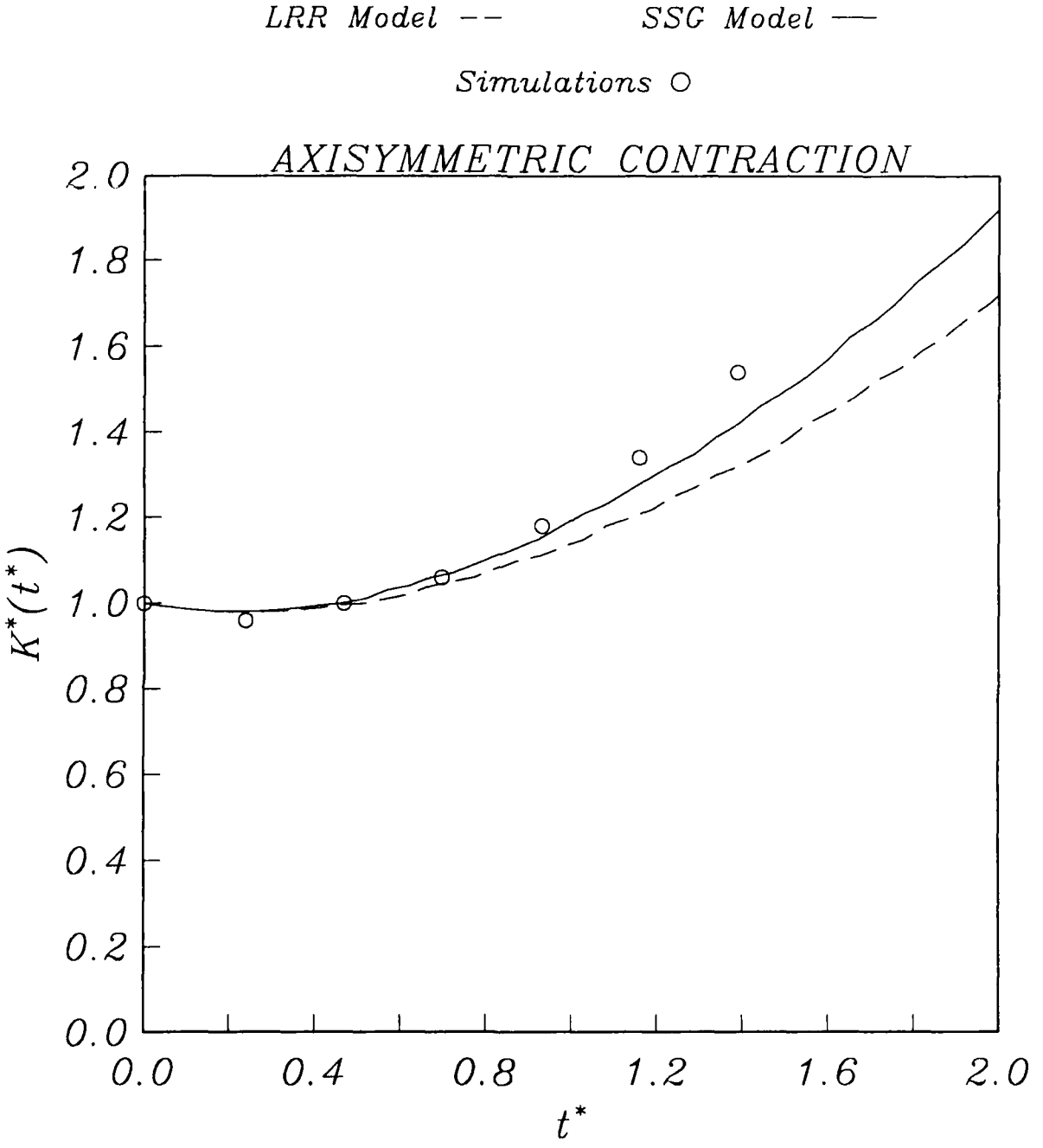

Figure 10. Time evolution of the turbulent kinetic energy in the axisymmetric contraction for $\varepsilon_0/SK_0 = 0.179$. Comparison of the predictions of the LRR model and SSG model with the direct simulations of Lee and Reynolds (1985).

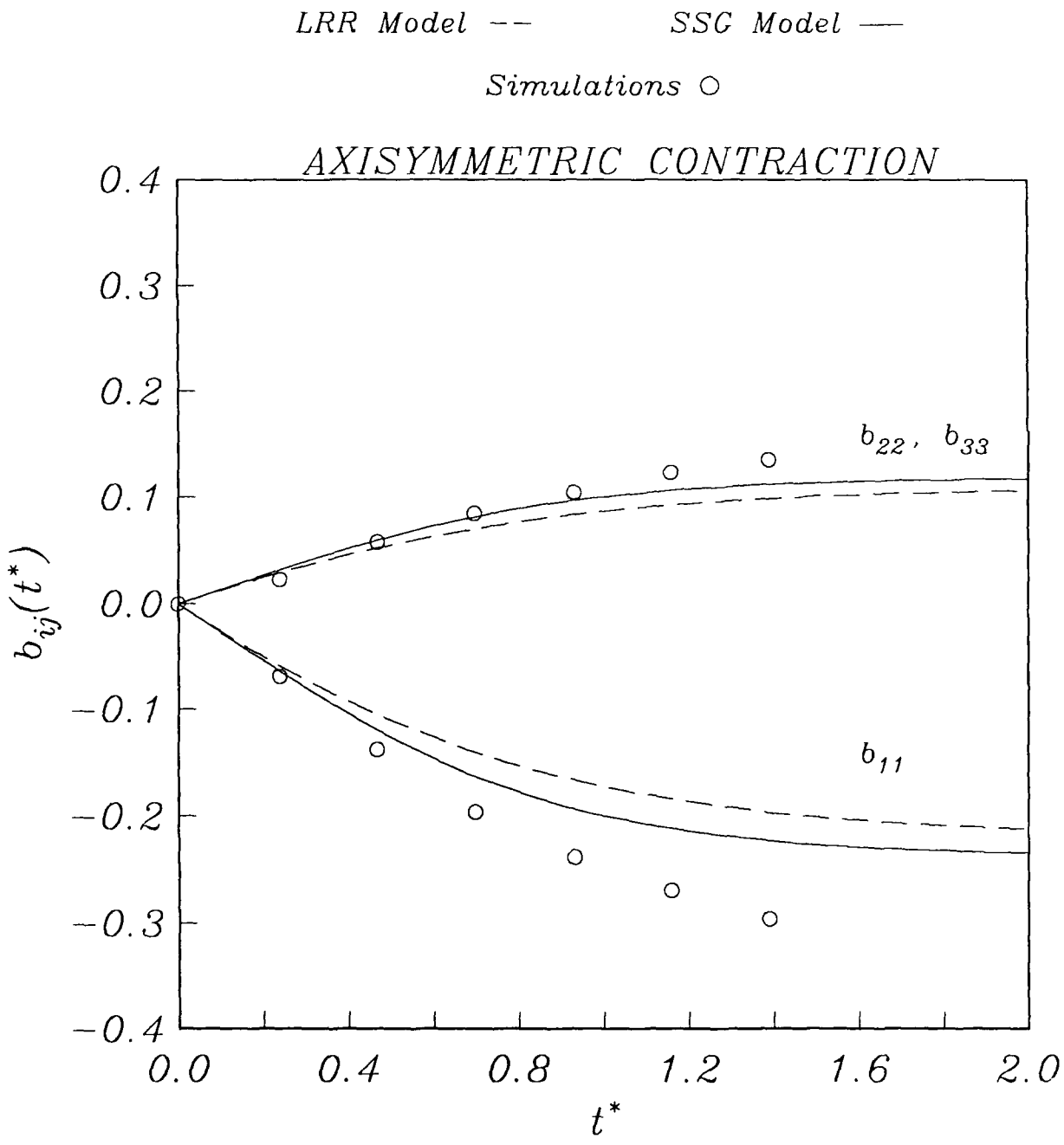

Figure 11. Time evolution of the anisotropy tensor in the axisymmetric contraction for $\varepsilon_0/SK_0 = 0.179$. Comparison of the predictions of the LRR model and SSG model with the direct simulations of Lee and Reynolds (1985).

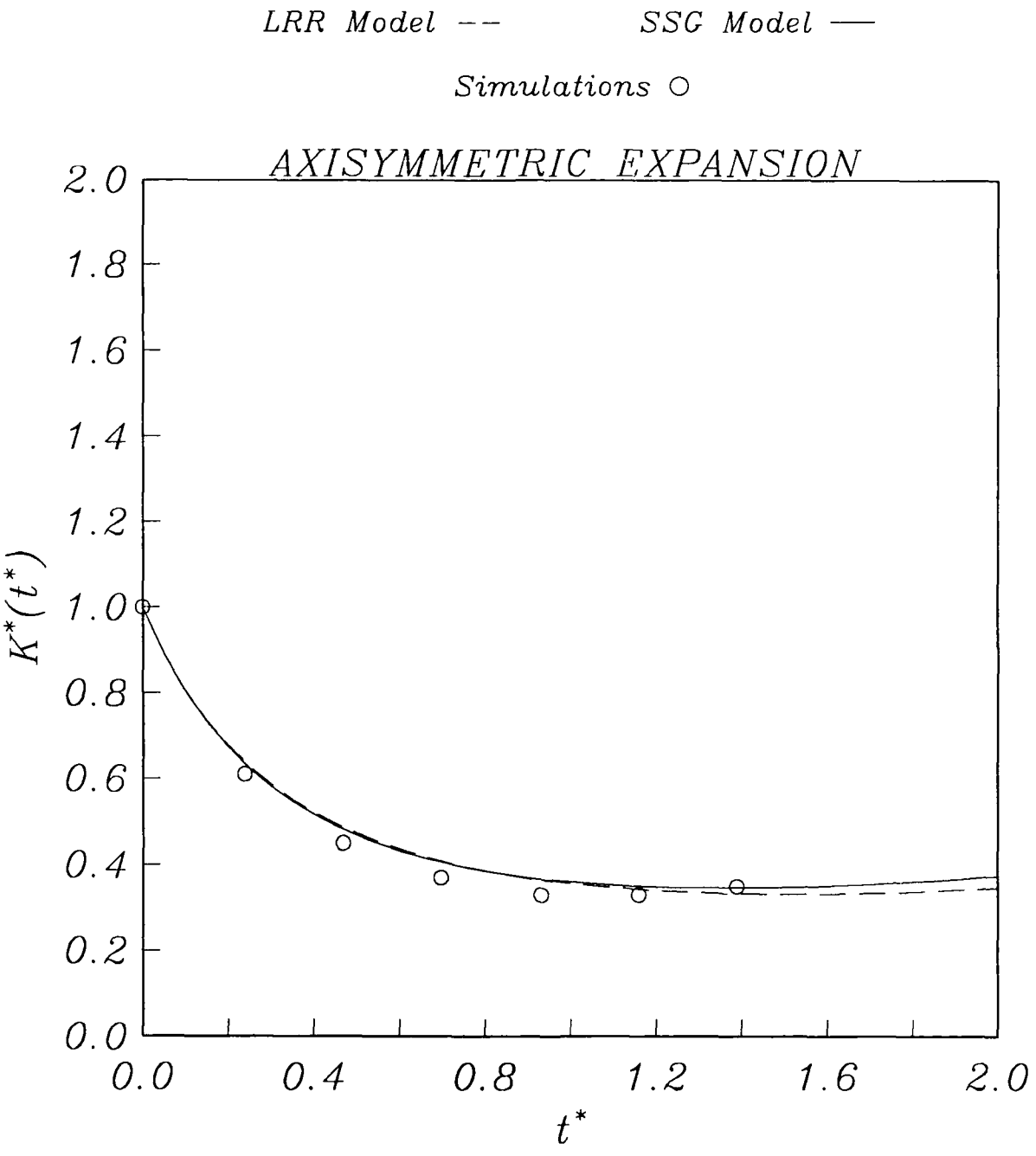

Figure 12. Time evolution of the turbulent kinetic energy in the axisymmetric expansion for $\varepsilon_0/SK_0 = 2.45$. Comparison of the predictions of the LRR model and SSG model with the direct simulations of Lee and Reynolds (1985).

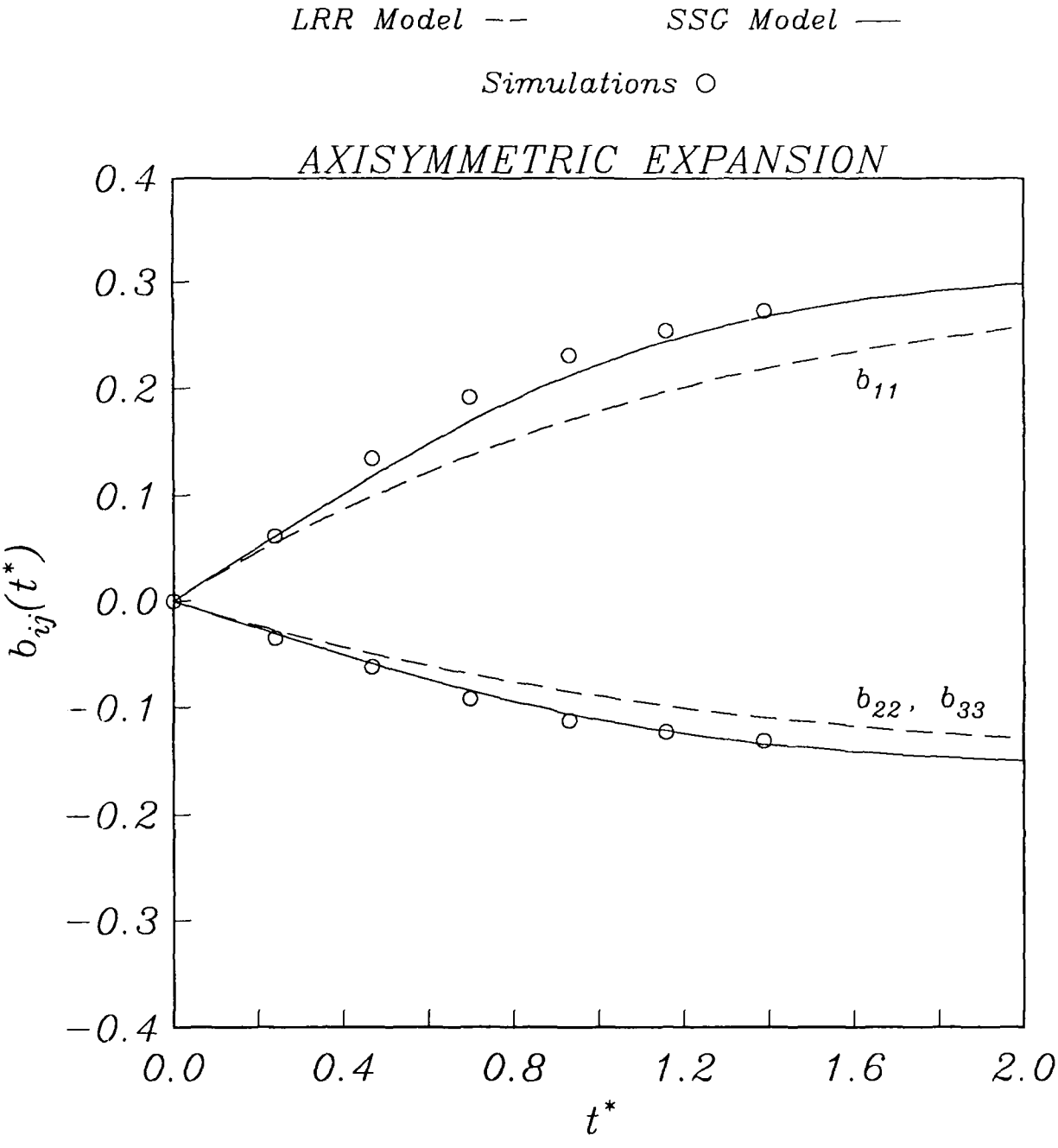

Figure 13. Time evolution of the anisotropy tensor in the axisymmetric expansion for $\varepsilon_0/SK_0 = 2.45$. Comparison of the predictions of the LRR model and SSG model with the direct simulations of Lee and Reynolds (1985).

Report Documentation Page

1. Report No.	2. Government Accession No.	3. Recipient's Catalog No.
NASA CR-181979 ICASE Report No. 90-5		

4. Title and Subtitle

MODELING THE PRESSURE-STRAIN CORRELATION OF TURBULENCE -- AN INVARIANT DYNAMICAL SYSTEMS APPROACH

5. Report Date

January 1990

6. Performing Organization Code

7. Author(s)

Charles G. Speziale
Sutanu Sarkar
Thomas B. Gatski

8. Performing Organization Report No.

90-5

10. Work Unit No.

505-90-21-01

9. Performing Organization Name and Address

Institute for Computer Applications in Science and Engineering
Mail Stop 132C, NASA Langley Research Center
Hampton, VA 23665-5225

11. Contract or Grant No.

NAS1-18605

13. Type of Report and Period Covered

Contractor Report

12. Sponsoring Agency Name and Address

National Aeronautics and Space Administration
Langley Research Center
Hampton, VA 23665-5225

14. Sponsoring Agency Code

15. Supplementary Notes

Langley Technical Monitor:
Richard W. Barnwell

Final Report

To be submitted to the Journal of Fluid Mechanics

16. Abstract

The modeling of the pressure-strain correlation of turbulence is examined from a basic theoretical standpoint with a view toward developing improved second-order closure models. Invariance considerations along with elementary dynamical systems theory are used in the analysis of the standard hierarchy of closure models. In these commonly used models, the pressure-strain correlation is assumed to be a linear function of the mean velocity gradients with coefficients that depend algebraically on the anisotropy tensor. It is proven that for plane homogeneous turbulent flows the equilibrium structure of this hierarchy of models is encapsulated by a relatively simple model which is only quadratically nonlinear in the anisotropy tensor. This new quadratic model - the SSG model - is shown to outperform the Launder, Reece, and Rodi model (as well as more recent models that have a considerably more complex nonlinear structure) in a variety of homogeneous turbulent flows. However, some deficiencies still remain for the description of rotating turbulent shear flows that are intrinsic to this general hierarchy of models and, hence, cannot be overcome by the mere introduction of more complex nonlinearities. It is thus argued that the recent trend of adding substantially more complex nonlinear terms containing the anisotropy tensor may by of questionable value in the modeling of the pressure-strain correlation. Possible alternative approaches are discussed briefly.

17. Key Words (Suggested by Author(s))	18. Distribution Statement
Turbulence Modeling; Second-Order Closure Models; Pressure-Strain Correlation; Homogeneous Turbulence	34 - Fluid Mechanics and Heat Transfer Unclassified - Unlimited

19. Security Classif. (of this report)	20. Security Classif. (of this page)	21. No. of pages	22. Price
Unclassified	Unclassified	52	A04

NASA FORM 1626 OCT 86